ACS OMEGA

Open Access

http://pubs.acs.org/journal/acsodf

Article

Discovery of 2-Pyrazolines That Inhibit the Phosphorylation of STAT3 as Nanomolar Cytotoxic Agents

Tejaswini P. Siddappa,[○] Akshay Ravish,[○] Zhang Xi, Arunkumar Mohan, Swamy S. Girimanchanaika, Niranjan Pattehali Krishnamurthy, Shreeja Basappa, Santosh L. Gaonkar, Peter E. Lobie, Vijay Pandey,* and Basappa Basappa*

Cite This: *ACS Omega* 2025, 10, 114−126

Read Online

ACCESS | Metrics & More | Article Recommendations | Supporting Information

ABSTRACT: STAT3 has emerged as a validated target in cancer, being functionally associated with breast cancer (BC) development, growth, resistance to chemotherapy, metastasis, and evasion of immune surveillance. Previously, a series of compounds consisting of imidazo[1,2-*a*]pyridine tethered 2-pyrazolines (referred to as ITPs) were developed that inhibit STAT3 phosphorylation in estrogen receptor-positive (ER+) BC cells. Herein, a new library of derivatives consisting of imidazo[1,2-*a*]pyridine clubbed 2-pyrazolines **2**(**a**−**o**) and its amide derivatives **3**(**a**−**af**) have been synthesized. Among these derivatives, **3n** and **3p** displayed efficacy to reduce ER+ BC cell viability, with IC_{50} values of 55 and 15 nM, respectively. Molecular docking simulations predicted that compound **3p** bound to STAT3 protein, with a binding energy of −9.56 kcal/mol. Using Western blot analysis, it was demonstrated that treatment of ER+ BC cells with compound **3p** decreased the levels of phosphorylated STAT3 at the Tyr705 residue. In conclusion, this investigation presents the synthesis of imidazopyridine clubbed 2-pyrazolines that exhibit significant efficacy in reducing viability of ER+ BC cells. In silico docking and Western blot analyses together support compound **3p** as a promising novel inhibitor of STAT3 phosphorylation, suggesting its potential as a valuable candidate for further therapeutic development.

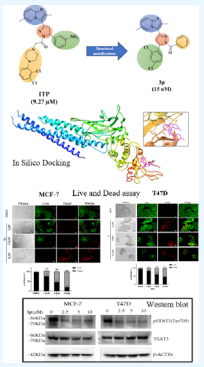

INTRODUCTION

Breast cancer (BC) ranks as the second leading cause of cancer-related death.[1] Treatment options for BC include surgical removal, chemotherapy, radiotherapy, and/or hormone therapy.[2−4] Reports have indicated that targeted therapeutics may effect dose reduction of traditional chemotherapy to reduce potential side effects.[5,6] STAT (signal transducer and activation of transcription) pathways exert potent roles in cellular functions and disease progression, and hence STATs may be designated as validated targets in oncology.[7] The STAT family comprises seven transcription factors—STAT1, STAT2, STAT3, STAT4, STAT5a, STAT5b, and STAT6.[8] STAT proteins contain specific functional domains including a terminal-NH_2 domain, a linker domain, a coiled-coil domain (CCD) that interacts with other proteins, an Src (short for sarcoma) homology 2 (SH2) domain (phosphorylation and dimerization), a DNA binding domain (DBD), and a C-terminal transactivation domain (TAD).[9,10]

STAT3 has garnered significant attention due to its positive association with development, growth, metastasis, chemoresistance, and immune evasion of cancer.[11−13] Indeed, numerous studies have documented the role of STAT3 in breast cancer, pertaining to disease progression and resistance to treatment.[14,15] Activation of the STAT3 pathway occurs in response to extracellular signals provided by cytokines (e.g., interleukins), growth factors (e.g., EGF, FGF), and hormones (e.g., growth hormone, leptin).[16] Upon binding to their respective receptors, these ligands initiate the activation of Janus (JAK) or other kinases, which, in turn, phosphorylate specific tyrosine residues on the receptor cytoplasmic domain, exposing docking site(s) for STAT3.[17] The phosphorylation of tyrosine 705 in STAT3 is required for activation of STAT3-mediated transcription. Once phosphorylated, STAT3 dissociates from the receptor/kinase complex, forming homodimers or heterodimers.[18,19] STAT3 dimers subsequently translocate from the cytoplasm to the nucleus. Within the nucleus, STAT3 initiates the transcription of genes associated with cell proliferation, survival, and motility.[20]

Heterocyclic molecules have gained interest due to their various pharmacological characteristics.[21−23] Pyrazolines, for example, hold promise as versatile molecules in drug development due to their pharmacological properties and possible therapeutic use.[24−27] Crizotinib (anticancer),[28] muzolimine (antihypertensive),[29] propyphenazone, ramifenazone (analgesic, antipyretic),[30] and phenylbutazone (analgesic)[31,32] are some of the pyrazole derivatives used clinically. Similarly, imidazopyridines such as zolpidem,[33] olprinone,[34]

Received: December 30, 2023
Revised: March 29, 2024
Accepted: April 3, 2024
Published: January 2, 2025

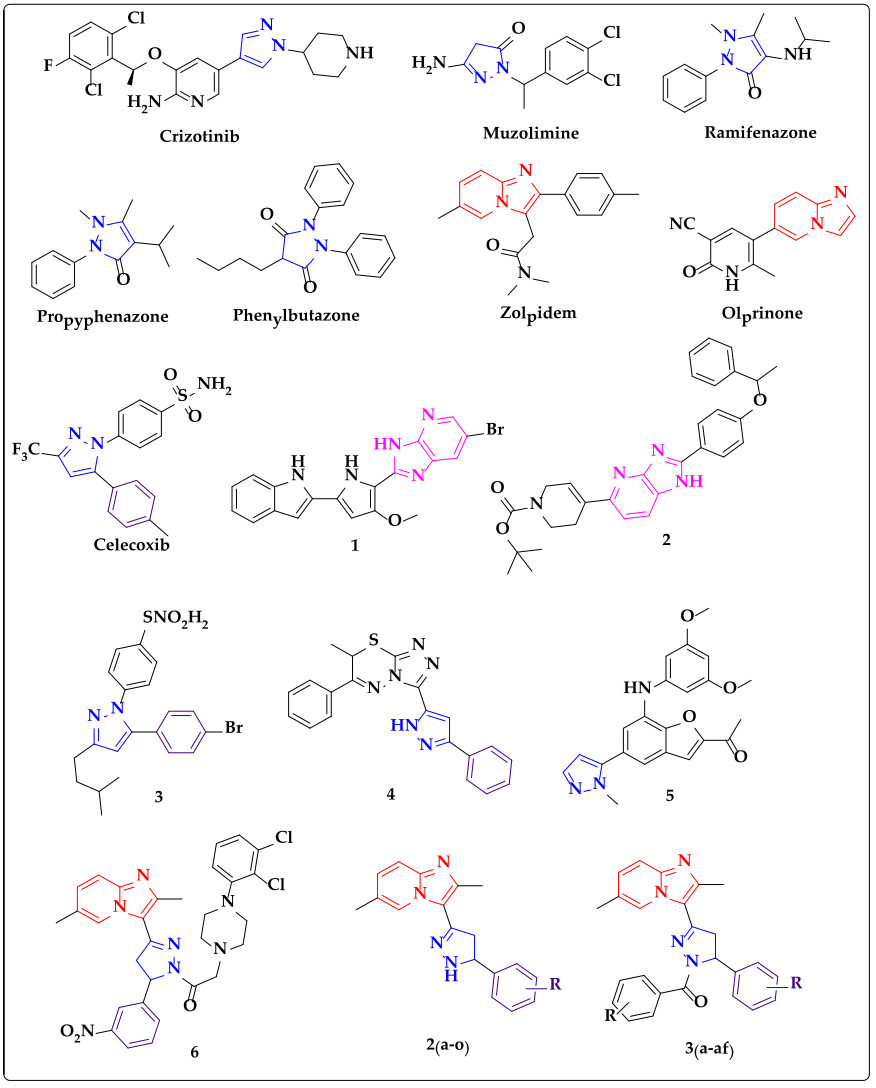

Figure 1. Structural overview of molecules containing imidazo[1,2-*a*]pyridine (red), imidazo[4,5-*b*]pyridine (pink), pyrazole/pyrazoline (blue), and aryl (purple) motifs as reported STAT3 inhibitors.

and zolimidine[35] have been demonstrated to possess anticancer activity (Figure 1).[36−38] It has been reported that imidazo[4,5-*b*]pyridine derivatives (**1**) reduce STAT3 activity by targeting SHP-1.[39] A novel and potent STAT3 inhibitor has been identified as disubstituted imidazo[4,5-*b*]pyridine (**2**) derivatives with *R* and *S* isomers. Additionally, the combination of **2** and gefitinib enhanced STAT3 inhibition.[40] A well-known pyrazole-containing drug (celecoxib) also suppresses STAT3 phosphorylation with resultant cell-cycle arrest and apoptosis of cancer cells.[41] Pyrazole derivatives (**3**) were reported to reduce STAT3 signaling in HGC cells in a dose-dependent manner and promote apoptosis.[42] Furthermore, 1,2,4-triazolo-[3,4-*b*]thiadiazine-clubbed pyrazoles (**4**) decrease phosphorylated STAT3 in cancer cells.[43] Benzofuran clubbed pyrazoles (**5**) also have been demonstrated to inhibit proliferation of MDA-MB-468 cells. Western blot analysis showed that compound **5** inhibited STAT3 (Tyr705) phosohorylation whereas it did not affect phosphorylation of STAT1 (Tyr701). Additionally, **5** induced significant G2/M cycle-arrest and early apoptosis in MDA-MB-468 cells in a concentration-dependent manner.[44]

In a previous report, we developed novel imidazo[1,2-*a*]pyridine tethered pyrazolines (ITPs) (**6**) and demonstrated their functional efficacy using human BC cells. Further characterization showed that the lead compound **6** inhibited STAT3 phosphorylation in estrogen receptor-positive (ER+) BC cells, namely MCF-7 and T47D. Compound **6** could also inhibit the nuclear translocation of STAT3 in MCF-7 and T47D.[45] We have previously synthesized pyrazoline-substituted piperazines and thiourea derivatives of pyrazolines. Herein, to explore the structural diversity of ITPs, newer pyrazolines and their amide derivatives **2**(**a**−**o**) and **3**(**a**−**af**) have been synthesized and their efficacy examined using determination of cell viability in MCF-7 cells. Among the series, **3n** and **3p** with IC_{50} values of 55 and 15 nM, respectively, exhibited more potent activity than other derivatives. The lead compound **3p** was predicted to bind to STAT3 protein with a binding energy of −9.56 kcal/mol using in silico analyses. Additionally, compound **3p** inhibited the phosphorylation of STAT3 (pSTAT3) in ER+ BC cells. This study indicates that compound **3p** and other derivatives exert potent activity against ER+ BC cells.

https://doi.org/10.1021/acsomega.3c10504
ACS Omega 2025, 10, 114−126

RESULTS

Synthesis of Pyrazoline Derivatives. The synthesis and pharmacological activities of imidazo[1,2-*a*]pyridin-2-ones as inhibitors of phospholipase A2 has been previously reported.[46] Furthermore, a new pyrazoline added imidazo[1,2-*a*]pyridine structure was reported as an inhibitor of STAT3 phosphorylation.[45] In this report, as detailed in materials and methods, pyrazolines and their amide derivatives have been synthesized (Scheme 1) and evaluated for loss of cell viability in MCF-7 cells, and the results are tabulated in Tables 1 and 2.

Scheme 1. Synthesis of Imidazopyridine Tethered Pyrazoline Derivatives[a]

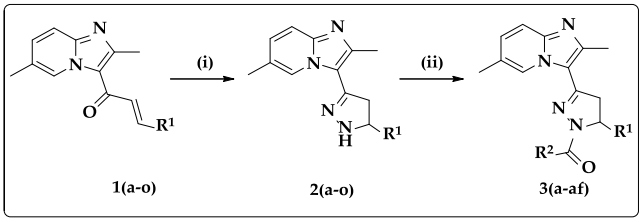

[a]R^1 = R^2 = aryl, heteroaryl. Reaction conditions: (i) hydrazine hydrate (1.5 mmol), EtOH, reflux, 8 h; (ii) substituted benzoyl chlorides (1.0 mmol), DCM, Et_3N, 0−5 °C, 30 min.

Table 1. List of Newly Synthesized Pyrazoline Derivatives 2(a−o) and Their Effect on Cell Viability in MCF-7 Cells

entry	R^1	IC_{50} (μM)
2a	4-nitrophenyl	23.63
2b	2,3,4-trimethoxyphenyl	28.47
2c	4-chlorophenyl	32.77
2d	4-bromophenyl	28.86
2e	4-fluorophenyl	>100
2f	3,4-dimethoxyphenyl	25.37
2g	thiophene	12.02
2h	3-fluorophenyl	11.65
2i	4-methoxyphenyl	>100
2j	4-methylphenyl	24.72
2k	3-hydroxy-4-methoxyphenyl	18.77
2l	2,4-dichlorophenyl	13.37
2m	3-hydroxyphenyl	13.49
2n	3-methoxyphenyl	20.98
2o	phenyl	>100
tamoxifen		1.75
doxorubicin		0.73

Efficacy of Pyrazoline Derivatives in Breast Cancer Cells. The newly synthesized pyrazolines were examined for their effect on cell viability in MCF-7 cells (Tables 1 and 2). Tamoxifen and doxorubicin were used as internal standards and produced loss of viability of MCF-7 cells with IC_{50} values of 1.75 and 0.73 μM, respectively (Figure 2). Among the series of compounds, **3n** and **3p** produced loss of cell viability of human breast cancer cells with IC_{50} values of 55 and 15 nM, respectively. Hence, it was observed that the dimethoxy and dichloro phenyl substituted compounds **3n** and **3p** are more potent than other structures. The IC_{50} values of the other derivatives lies between 3.65 and >100 μM (Supporting Information). The lead compound **3p** was also examined for effects on cell viability in MCF10A cells (immortalized mammary epithelial cells). In this cell line, compound **3p**

Table 2. List of Newly Synthesized Pyrazoline Amide Derivatives 3(a−af) and Their Effect on Cell Viability in MCF-7 Cells

entry	R^1	R^2	IC_{50} (μM)
3a	2,3,4-trimethoxyphenyl	3-fluorophenyl	>100
3b	4-chlorophenyl	3-fluorophenyl	39.46
3c	4-bromophenyl	3-fluorophenyl	4.44
3d	4-fluorophenyl	3-fluorophenyl	11.86
3e	4-fluorophenyl	phenyl	89.41
3f	4-fluorophenyl	3-methoxyphenyl	95.30
3g	4-fluorophenyl	4-methoxyphenyl	>100
3h	4-fluorophenyl	3,5-dinitrophenyl	57.76
3i	4-fluorophenyl	2-fluorophenyl	>100
3j	3,4-dimethoxyphenyl	3-fluorophenyl	16.31
3k	3,4-dimethoxyphenyl	phenyl	42.87
3l	3,4-dimethoxyphenyl	3,5-dinitrophenyl	47.06
3m	3,4-dimethoxyphenyl	3-methoxyphenyl	>100
3n	3,4-dimethoxyphenyl	4-methoxyphenyl	0.055
3o	2,4-dichlorophenyl	3-fluorophenyl	5.72
3p	2,4-dichlorophenyl	phenyl	0.015
3q	2,4-dichlorophenyl	3,5-dinitrophenyl	>100
3r	2,4-dichlorophenyl	3-methoxyphenyl	>100
3s	2,4-dichlorophenyl	2-fluorophenyl	7.48
3t	2,4-dichlorophenyl	4-methoxyphenyl	>100
3u	4-nitrophenyl	3-fluorophenyl	76.93
3v	4-nitrophenyl	phenyl	16.56
3w	4-nitrophenyl	2-fluorophenyl	>100
3x	4-nitrophenyl	2,6-difluorophenyl	>100
3y	thiophene	3-fluorophenyl	43.94
3z	3-fluorophenyl	3-fluorophenyl	17.64
3aa	4-methoxyphenyl	3-fluorophenyl	17.67
3ab	4-methylphenyl	3-fluorophenyl	3.65
3ac	3-hydroxy-4-methoxyphenyl	3-fluorophenyl	24.18
3ad	3-hydroxyphenyl	3-fluorophenyl	47.14
3ae	3-methoxyphenyl	3-fluorophenyl	28.63
3af	phenyl	3-fluorophenyl	11.71
tamoxifen			1.75
doxorubicin			0.73

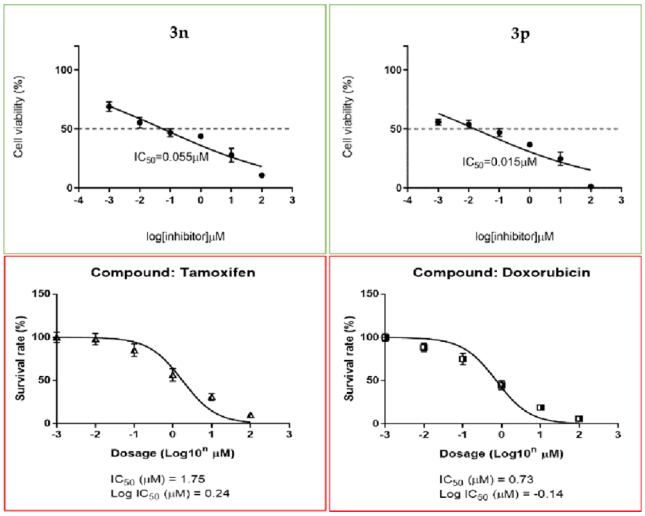

Figure 2. IC_{50} curves for the active compounds **3n** and **3p** (green) with tamoxifen and doxorubicin (red) as reference drugs against MCF-7 cells.

https://doi.org/10.1021/acsomega.3c10504
ACS Omega 2025, 10, 114−126

exhibited an IC_{50} of 125.1 μM, indicating that the compound is potentially less effective in nononcogenically transformed cells.

In Silico Analysis of Compound 3p Targeting STAT3. To determine the predicted binding affinity and the critical interactions of compound **3p** (R enantiomer) with the SH2 domain of STAT3 (PDB ID: 1BG1), in silico analysis was performed using AutoDock4 tools. The binding energy of **3p** was calculated to be −9.56 kcal/mol compared with the previously reported ITP compounds (Structure 6, Figure 1) of −9.27 kcal/mol.[45] The SH2 domain of STAT3 possesses three pockets pY, pY+1, and pY−X. In silico docking analysis revealed that compound **3p** could potentially bind to the pY binding pocket of the SH2 domain. The *N* of the imidazopyridine ring formed two hydrogen bonds with Arg-609 with a bond distance of 2.058 and 2.199 Å. Hydrophobic interactions were observed with residue Lys-591, Arg-595, Ile-634, Gln-635 (π-sigma), and Pro-639, which further enhanced the stability of protein−ligand complex.(Figure 3)

Compound 3p Inhibited pStat3 Levels in MCF-7 and T47D Cells. The activation of STAT3 requires phosphorylation at sites in the SH2 domain and transactivation domain at Tyr705.[47] Compound **3p** was therefore assessed for its effects on pSTAT3-Tyr705 levels in MCF-7 and T47D cells using Western blot analysis. It was observed that treatment of these cells with compound **3p** resulted in significantly decreased levels of pSTAT3-Tyr705 compared to vehicle-treated control cells (Figure 4). These findings are consistent with the in silico prediction of compound **3p** binding to STAT3.

Live/Dead Cell Assay. The potential effect of compound **3p** on cell survival was examined using a live/dead cell assay in MCF-7 (Figure 5) and T47D cells (Figure 6). Upon treatment with compound **3p**, both MCF-7 and T47D cells exhibited a dose-dependent increase in cell death. Furthermore, up to 80% of MCF-7 cells were categorized as dead after treatment with compound **3p** at a 5 μM dose. Treatment of T47D cells with compound **3p** produced 60% cell death.

DISCUSSION

STAT3 is a validated target in oncology. Targeting the STAT3-SH2 domain allows for the inhibition of phosphorylation of Tyr705 of STAT3, which is required for STAT3-related signaling in cancer cells.[48] The SH2 domain of STAT3 contains three pockets, namely pY, pY+1, and pY−X.[49] Tyr705 is located in the pY pocket of the SH2 domain.[50,51] With this consideration, the synthesis and efficacy of tetrahydropyridine-pyrazoles as inhibitors of STAT3 phosphorylation was previously reported.[52] Furthermore, a novel azaspirane structure was also previously reported as an inhibitor of the JAK-STAT pathway in vivo.[53] Later, imidazopyridine-tethered pyrazolines (ITPs) that target pSTAT3 at Tyr706 and Ser727 in MCF-7 and T47D cells were developed.[45] Pyrazole-based hybrid structures were reported to be an inhibitor of STAT3 phosphorylation and these molecules were optimized via a structure-based approach.[54] Recently, pyrazole-based compounds were also reported as anticancer agents that inhibited STAT3-related pathways in BC cells.[54−56] In the present work, the aim was to synthesize novel pyrazolines that could potentially target the SH2 domain of STAT3. The newly synthesized 2-pyrazolines (**3p** and **3n**) inhibited the viability of MCF-7 cells in the nanomolar range. As predicted by in silico analysis, compound **3p** also inhibited the phosphorylation of Tyr705 in MCF-7 and T47D cells. Compared to the previously reported ITPs, compound **3p** exhibited potent efficacy associated with a higher binding energy toward STAT3 (in silico data). Hence, the present study demonstrated that compound **3p**, identified in this report, provides a novel chemical structure that may be further optimized to develop STAT3 inhibitors for use in oncology.

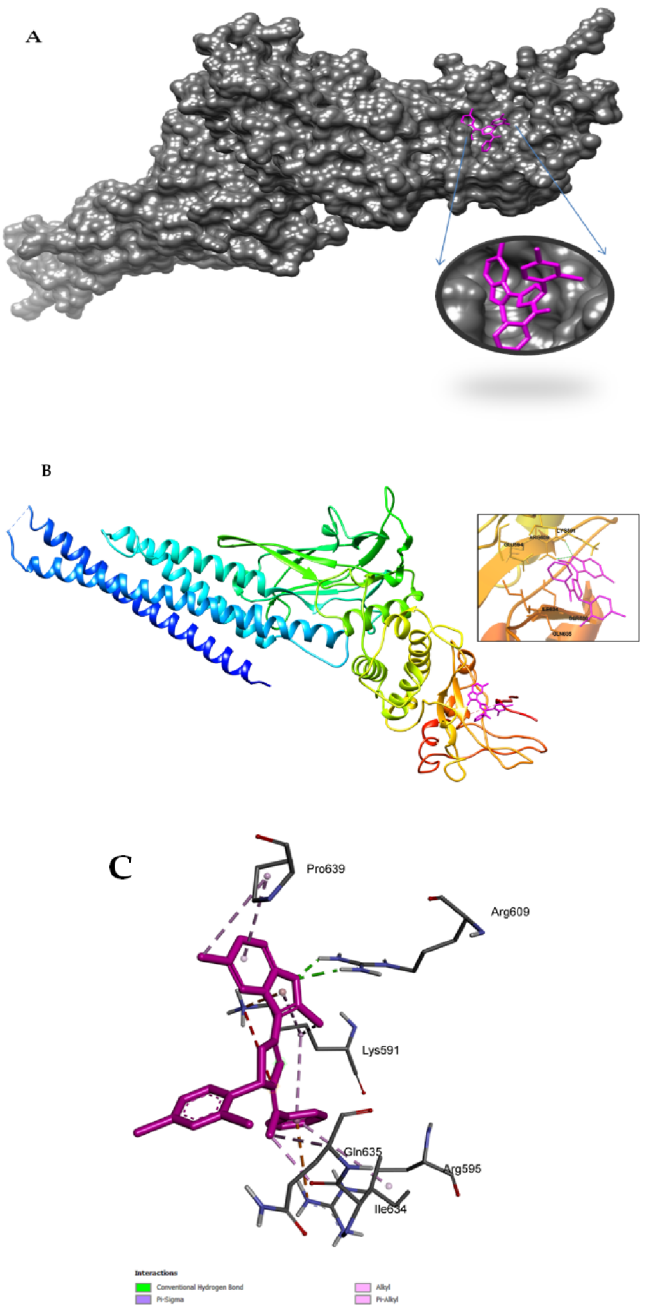

Figure 3. (A) 3D surface view of docked compound **3p** (pink) inside the pY binding pocket of the SH2 domain of STAT3. (B) Cartoon representation of **3p** and hydrogen bonding interaction with Arg609. (C) **3p** showing detailed interactions with amino acids of the SH2 domain.

MATERIALS AND METHODS

All chemicals and solvents for compound synthesis were obtained from Sigma-Aldrich (Bangalore, India). The reactions were monitored by precoated silica gel thin-layer chromatography (TLC) plates. ^{1}H and ^{13}C NMR were recorded on an

https://doi.org/10.1021/acsomega.3c10504
ACS Omega 2025, 10, 114−126

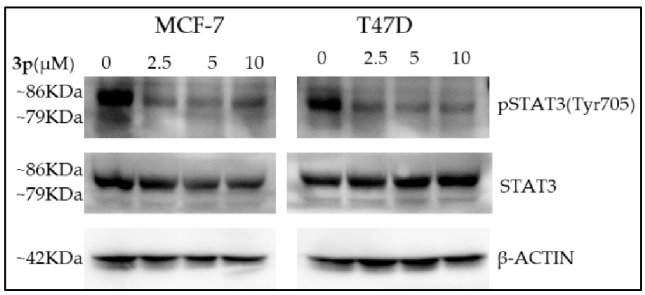

Figure 4. Compound **3p** inhibits STAT3 phosphorylation in MCF-7 and T47D cells in a concentration-dependent manner. MCF-7 and T47D cells were treated for 24 h with the indicated concentrations of **3p** at 0, 2.5, 5, and 10 μM. β-ACTIN was used as input control.

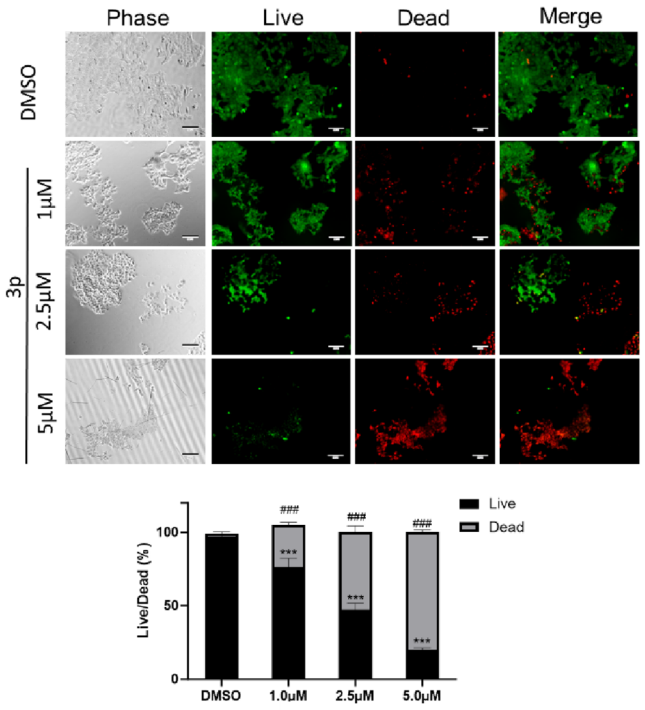

Figure 5. Live/dead cell assay in MCF-7 cancer cells. After treatment with **3p** (0, 1, 2.5, and 5 μM), the cells were stained with calcein AM and EthD-1 for 30 min at 37 °C, and then the live/dead cells were determined by fluorescence microscopy. Black region represents percentage of live cells and gray region represents percentage of dead cells.

Agilent NMR spectrophotometer (400 or 500 MHz). TMS and DMSO or $CDCl_3$ were used as an internal standard and solvent, respectively, and chemical shifts were expressed as ppm (Santa Clara, CA, USA). Bruker Daltonics equipment was used to determine high-resolution mass spectra.

Synthesis of Compounds 3(a−af). As per our previous report,[45] four different chalcones **1(a−o)** were synthesized. Further, compounds **2(a−o)** were synthesized by refluxing chalcones and hydrazine hydrate in ethanol for 8 h. The completion of the reaction was monitored by thin-layer chromatography. Upon reaction completion, the solid reaction mixture was filtered off, washed with water, dried, and used for the next step without purification. To a stirred solution of **2(a−o)** in DCM, triethylamine (2−3 drops) and various substituted benzoyl chlorides were added and stirring was further continued for 15 min at 0−5 °C. After the completion

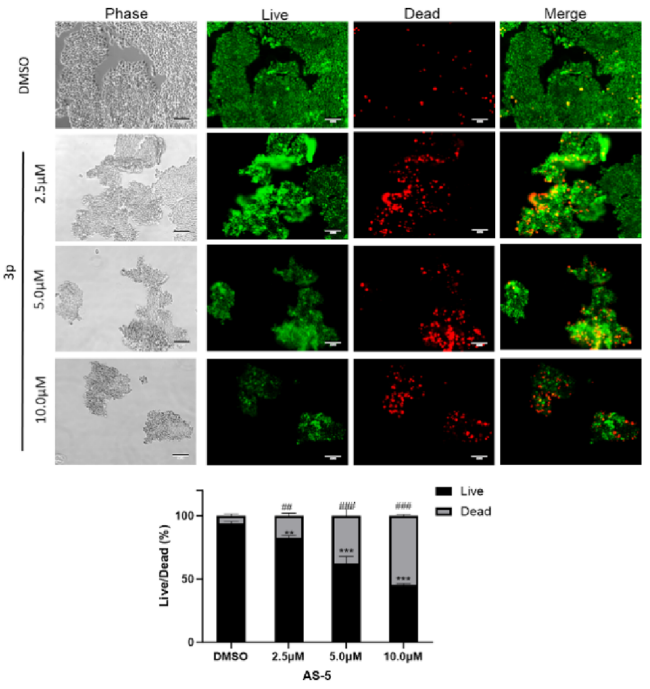

Figure 6. Live/dead cell assay in T47D cells. After treatment with **3p** (0, 2.5, 5, and 10 μM), the cells were stained with calcein AM and EthD-1 for 30 min at 37 °C, and then the live/dead cells were determined by fluorescence microscopy. Black region represents percentage of live cells and gray region represents percentage of dead cells.

of the reaction, the desired product from the reaction mixture was obtained after solvent extraction (DCM:water), and further purification was achieved by recrystallization using ethyl acetate and hexane as solvent. The newly synthesized molecules were characterized by melting point, NMR, and mass spectrometry. The NMR and mass spectra are included in the Supporting Information file.

Spectral Data. *2,6-Dimethyl-3-(5-(4-nitrophenyl)-4,5-dihydro-1H-pyrazol-3-yl)imidazo[1,2-a]pyridine (2a).* Yellow solid; MP: 152−154 °C; yield: 80%; ^{1}H NMR (500 MHz, $CDCl_3$) δ 9.30 (s, 1H, Ar−H), 8.22 (d, J = 8.7 Hz, 2H, Ar−H), 7.61 (d, J = 8.7 Hz, 2H, Ar−H), 7.48 (d, J = 9.0 Hz, 1H, Ar−H), 7.14 (dd, J = 9.0, 1.3 Hz, 1H, Ar−H), 6.06 (s, 1H, NH), 5.01 (t, J = 10.1 Hz, 1H, CH), 3.77 (dd, J = 15.9, 10.5 Hz, 1H, CH_2), 3.19 (dd, J = 15.9, 9.7 Hz, 1H, CH_2), 2.57 (s, 3H, CH_3), 2.38 (s, 3H, CH_3); ^{13}C NMR (100 MHz, $CDCl_3$) δ 149.73, 147.67, 144.71, 129.22, 128.78, 128.58, 127.60, 127.35, 126.35, 124.27, 122.99, 115.60, 62.71 (CH), 44.52 (CH_2), 18.58 (CH_3), 16.14 (CH_3); mass spectra: calculated for $C_{18}H_{17}N_5O_2$ = 335.3599; observed = 336.1850 $[M + H]^+$.

2,6-Dimethyl-3-(5-(3,4,5-trimethoxyphenyl)-4,5-dihydro-1H-pyrazol-3-yl)imidazo[1,2-a] pyridine (2b). White solid; MP: 102−104 °C; yield: 82%; ^{1}H NMR (400 MHz, $CDCl_3$): δ 9.32 (s, 1H, Ar−H), 7.48 (d, J = 9.1 Hz, 1H, Ar−H), 7.13 (d, J = 9.1 Hz, 1H, Ar−H), 6.67 (s, 2H, Ar−H), 5.98 (s, 1H, NH), 4.84 (t, J = 10.3 Hz, 1H, CH), 3.86 (s, 6H, $(OCH_3)_2$), 3.84 (s, 3H, OCH_3), 3.70−3.64 (m, 1H, CH_2), 3.20 (dd, J = 15.9, 10.4 Hz, 1H, CH_2), 2.59 (s, 3H, CH_3), 2.37 (s, 3H, CH_3); ^{13}C NMR (100 MHz, $CDCl_3$) δ 153.62, 145.23, 145.02, 144.90, 137.88, 137.54, 128.78, 126.31, 122.68, 115.61, 114.77, 103.44, 63.95 (CH), 60.96 (OCH_3), 56.26 (OCH_3), 44.67 (CH_2),

https://doi.org/10.1021/acsomega.3c10504
ACS Omega 2025, 10, 114−126

18.59 (CH_3), 16.24 (CH_3); mass spectra: calculated for $C_{21}H_{24}N_4O_3$ = 380.1848; observed = 381.1978 $[M + H]^+$.

3-(5-(4-Chlorophenyl)-4,5-dihydro-1H-pyrazol-3-yl)-2,6-dimethylimidazo[1,2-a]pyridine (2c). White solid; MP: 164−166 °C; yield: 97%; ^{1}H NMR (400 MHz, $CDCl_3$): δ 9.31 (s, 1H, Ar−H), 7.48 (d, J = 9.0 Hz, 1H, Ar−H), 7.33 (q, J = 8.5 Hz, 4H, Ar−H), 7.13 (d, J = 9.0 Hz, 1H, Ar−H), 5.96 (s, 1H, NH), 4.87 (t, J = 9.7 Hz, 1H, CH), 3.68 (dd, J = 15.9, 10.4 Hz, 1H, CH_2), 3.19 (dd, J = 15.8, 9.1 Hz, 1H, CH_2), 2.58 (s, 3H, CH_3), 2.37 (s, 3H, CH_3); ^{13}C NMR (100 MHz, $CDCl_3$) δ 145.03, 144.91, 140.96, 133.70, 129.12, 128.91, 127.94, 126.35, 122.72, 115.61, 114.69, 62.71 (CH), 44.37 (CH_2), 18.57 (CH_3), 16.22 (CH_3).

3-(5-(4-Bromophenyl)-4,5-dihydro-1H-pyrazol-3-yl)-2,6-dimethylimidazo[1,2-a]pyridine (2d). Yellow solid; MP: 148−150 °C; yield: 97%; ^{1}H NMR (400 MHz, $CDCl_3$): δ 9.30 (s, 1H, Ar−H), 7.47 (dd, J = 8.8, 2.4 Hz, 3H, Ar−H), 7.29 (d, J = 8.3 Hz, 2H, Ar−H), 7.13 (d, J = 8.9 Hz, 1H, Ar−H), 5.95 (s, 1H, NH), 4.86 (t, J = 9.7 Hz, 1H, CH), 3.69 (dd, J = 15.8, 10.4 Hz, 1H, CH_2), 3.19 (dd, J = 15.9, 9.1 Hz, 1H, CH_2), 2.58 (s, 3H, CH_3), 2.37 (s, 3H, CH_3); ^{13}C NMR (100 MHz, $CDCl_3$) δ 145.03, 144.89, 141.48, 132.07, 128.93, 128.29, 126.35, 122.73, 121.77, 120.75, 115.60, 62.75 (CH), 44.33 (CH_2), 18.56 (CH_3), 16.20 (CH_3); mass spectra: calculated for $C_{18}H_{17}BrN_4$ = 368.0637; observed = 369.0789 $[M + H]^+$.

3-(5-(4-Fluorophenyl)-4,5-dihydro-1H-pyrazol-3-yl)-2,6-dimethylimidazo[1,2-a]pyridine (2e). Yellow solid; MP: 150−152 °C; yield = 95%; ^{1}H NMR (400 MHz, $CDCl_3$): δ 9.31 (s, 1H, Ar−H), 7.47 (d, J = 9.0 Hz, 1H, Ar−H), 7.38 (dd, J = 8.4, 5.5 Hz, 2H, Ar−H), 7.13 (d, J = 9.1 Hz, 1H, Ar−H), 7.04 (t, J = 8.6 Hz, 2H, Ar−H), 4.88 (t, J = 9.7 Hz, 1H, NH), 3.68 (dd, J = 15.9, 10.2 Hz, 1H, CH_2), 3.23−3.17 (m, 1H, CH_2), 2.58 (s, 3H, CH_3), 2.37 (s, 3H, CH_3); ^{13}C NMR (100 MHz, $CDCl_3$) δ 163.43, 161.47, 145.06, 144.98, 144.92, 138.23, 128.88, 128.18, 126.35, 122.66, 115.64, 114.74, 62.74, 62.66 (CH), 44.41 (CH_2), 18.56 (CH_3), 16.22 (CH_3); mass spectra: calculated for $C_{18}H_{17}FN_4$ = 308.1437; observed = 309.1589 $[M + H]^+$.

3-(5-(3,4-Dimethoxyphenyl)-4,5-dihydro-1H-pyrazol-3-yl)-2,6-dimethylimidazo[1,2-a]pyridine (2f). Yellow solid; MP: 150−152 °C; yield = 90%; ^{1}H NMR (400 MHz, $CDCl_3$): δ 9.32 (s, 1H, Ar−H), 7.47 (d, J = 9.1 Hz, 1H, Ar−H), 7.12 (d, J = 9.1 Hz, 1H, Ar−H), 6.99 (d, J = 1.1 Hz, 1H, Ar−H), 6.93 (d, J = 8.3 Hz, 1H, Ar−H), 6.83 (d, J = 8.2 Hz, 1H, Ar−H), 4.85 (t, J = 9.9 Hz, 1H, NH), 3.87 (s, 6H, $((OCH_3)_2)$, 3.65 (dd, J = 15.9, 10.2 Hz, 1H, CH), 3.21 (dd, J = 15.8, 9.7 Hz, 1H, CH), 2.59 (s, 3H, CH_3), 2.36 (s, 3H, CH_3); ^{13}C NMR (100 MHz, $CDCl_3$) δ 149.37, 148.80, 145.19, 144.98, 144.87, 134.80, 128.77, 126.34, 122.61, 118.84, 115.60, 114.85, 111.29, 109.42, 63.36 (CH), 56.06 (CH_3), 56.02 (CH_3), 44.47 (CH_2), 18.55 (CH_3), 16.22 (CH_3); mass spectra: calculated for $C_{20}H_{22}N_4O_2$ = 350.1743; observed = 351.1892 $[M + H]^+$.

3-(5-(3-Fluorophenyl)-4,5-dihydro-1H-pyrazol-3-yl)-2,6-dimethylimidazo[1,2-a]pyridine (2h). Brown solid; MP: 106−108 °C: ^{1}H NMR (400 MHz, DMSO-d_6) δ 9.26 (s, 1H, Ar−H), 8.98 (s, 1H, Ar−H), 7.52−7.39 (m, 2H, Ar−H), 7.21 (d, J = 9.0 Hz, 1H, Ar−H), 6.87 (s, 2H, Ar−H), 6.79 (d, J = 8.0 Hz, 1H, NH), 4.69 (t, J = 10.2 Hz, 1H, CH), 3.62 (dd, J = 15.6, 10.5 Hz, 1H, CH_2), 3.02 (dd, J = 15.5, 10.7 Hz, 1H, CH_2), 2.50 (s, 3H, CH_3), 2.34 (s, 3H, CH_3); ^{13}C NMR (100 MHz, DMSO-d_6) δ 147.39, 147.00, 144.32, 144.03, 143.07, 135.84, 128.41, 125.65, 122.38, 117.85, 115.83, 115.13, 114.33, 112.62, 62.76 (CH), 56.18 (CH_2), 18.49 (CH_3), 16.17 (CH_3).

3-(5-(4-Methoxyphenyl)-4,5-dihydro-1H-pyrazol-3-yl)-2,6-dimethylimidazo[1,2-a]pyridine (2i). Brown solid; MP: 108−110 °C; yield: 75%; ^{1}H NMR (400 MHz, DMSO-d_6) δ 9.27 (s, 1H, Ar−H), 7.48 (d, J = 7.6 Hz, 2H, Ar−H), 7.36 (d, J = 6.4 Hz, 2H, Ar−H), 7.21 (d, J = 7.9 Hz, 1H, Ar−H), 6.92 (d, J = 6.4 Hz, 2H, Ar−H, NH), 4.77 (s, 1H, CH), 3.74 (s, 3H, OCH_3), 3.70−3.60 (m, 1H, CH_2), 3.11−3.00 (m, 1H, CH_2), 2.50 (s, 3H, CH_3), 2.34 (s, 3H, CH_3); ^{13}C NMR (100 MHz, DMSO-d_6) δ 158.97, 144.36, 144.05, 143.26, 134.93, 128.46, 128.39, 125.66, 122.41, 115.82, 115.10, 114.25, 62.72 (CH), 55.55 (OCH_3), 18.47 (CH_3), 16.15 (CH_3); mass spectra: calculated for $C_{19}H_{20}N_4O$ = 321.1637; observed = 322.1646 $[M + H]^+$.

3-(5-(4-Methoxyphenyl)-4,5-dihydro-1H-pyrazol-3-yl)-2,6-dimethylimidazo[1,2-a]pyridine (2j). White solid; MP: 122−124 °C; ^{1}H NMR (400 MHz, DMSO-d_6) δ 9.27 (s, 1H, Ar−H), 7.48 (d, J = 9.1 Hz, 1H, Ar−H), 7.32 (d, J = 7.7 Hz, 2H, Ar−H), 7.18 (dd, J = 18.7, 8.4 Hz, 3H, Ar−H), 4.78 (t, J = 10.6 Hz, 1H, CH), 3.67 (dd, J = 15.8, 10.4 Hz, 1H, CH_2), 3.05 (dd, J = 15.7, 11.0 Hz, 1H, CH_2), 2.50 (s, 3H, OCH_3), 2.34 (s, 3H, CH_3), 2.29 (s, 3H, CH_3); ^{13}C NMR (100 MHz, DMSO-d_6) δ 144.39, 144.06, 143.20, 140.10, 136.73, 129.40, 128.42, 127.16, 125.66, 122.39, 115.85, 115.08, 62.94 (CH), 43.67 (CH_2), 21.16 (CH_3), 18.48 (CH_3), 16.18 (CH_3).

5-(3-(2,6-Dimethylimidazo[1,2-a]pyridin-3-yl)-4,5-dihydro-1H-pyrazol-5-yl)-2-methoxyphenol (2k). Brown solid; MP: 112−114 °C; yield: 97%; ^{1}H NMR (400 MHz, DMSO-d_6) δ 9.26 (s, 1H, Ar−H), 9.00 (s, 1H, Ar−H), 7.49 (d, J = 9.0 Hz, 1H, Ar−H), 7.21 (d, J = 9.0 Hz, 1H, Ar−H), 6.87 (d, J = 6.9 Hz, 2H, Ar−H), 6.79 (d, J = 8.1 Hz, 1H, NH), 4.69 (t, J = 10.2 Hz, 1H, CH), 3.24 (s, 3H, OCH_3), 3.62 (dd, J = 15.6, 10.5 Hz, 1H, CH_2), 3.02 (dd, J = 15.5, 10.7 Hz, 1H, CH_2), 2.50 (s, 3H, CH_3), 2.34 (s, 3H, CH_3); ^{13}C NMR (100 MHz, DMSO-d_6) δ 147.38, 146.98, 144.32, 144.02, 143.08, 135.81, 128.44, 125.65, 122.40, 117.85, 115.82, 115.12, 114.31, 112.58, 62.76 (CH), 56.16 (OCH_3), 43.74 (CH_2), 18.49 (CH_3), 16.16 (CH_3).

3-(5-(2,4-Dichlorophenyl)-4,5-dihydro-1H-pyrazol-3-yl)-2,6-dimethylimidazo[1,2-a]pyridine (2l). Yellow solid; MP: 136−138 °C; ^{1}H NMR (400 MHz, DMSO-d_6) δ 9.25 (s, 1H, Ar−H), 7.64 (dd, J = 18.3, 6.4 Hz, 3H, Ar−H), 7.46 (dd, J = 13.2, 8.8 Hz, 2H, Ar−H), 7.21 (d, J = 9.0 Hz, 1H, NH), 5.08 (td, J = 10.3, 3.3 Hz, 1H, CH), 3.81 (dd, J = 16.0, 10.8 Hz, 1H, CH_2), 3.00 (dd, J = 16.0, 10.0 Hz, 1H, CH_2), 2.48 (s, 3H, CH_3), 2.34 (s, 3H, CH_3); ^{13}C NMR (100 MHz, DMSO-d_6) δ 144.68, 144.15, 143.00, 139.91, 133.34, 132.85, 129.83, 129.17, 128.60, 128.06, 125.67, 122.52, 115.83, 114.79, 59.28 (CH), 42.40 (CH_2), 18.48 (CH_3), 16.14 (CH_3); mass spectra: calculated for $C_{18}H_{16}Cl_2N_4$ = 358.0752; observed = 359.0888 $[M + H]^+$.

3-(3-(2,6-Dimethylimidazo[1,2-a]pyridin-3-yl)-4,5-dihydro-1H-pyrazol-5-yl)phenol (2m). Yellow solid; MP: 156−158 °C; ^{1}H NMR (400 MHz, DMSO-d_6): δ 9.41 (s, 1H, Ar−OH), 9.27 (s, 1H, Ar−H), 7.48 (d, J = 9.3 Hz, 2H, Ar−H), 7.24−7.10 (m, 2H, Ar−H), 6.85 (d, J = 8.6 Hz, 1H, Ar−H), 6.67 (d, J = 7.3 Hz, 1H, NH), 4.74 (t, J = 10.1 Hz, 1H, CH), 3.67 (dd, J = 15.2, 10.9 Hz, 1H, CH_2), 3.05 (dd, J = 15.0, 11.1 Hz, 1H, CH_2), 2.50 (s, 3H, CH_3), 2.34 (s, 3H, CH_3); ^{13}C NMR (100 MHz, DMSO-d_6) δ 157.94, 144.78, 144.38, 144.05, 143.08, 129.84, 128.43, 125.66, 122.39, 117.84, 115.83, 115.08, 114.62, 113.89, 63.06 (CH), 43.71 (CH_2), 18.48 (CH_3), 16.16

https://doi.org/10.1021/acsomega.3c10504
ACS Omega 2025, 10, 114−126

(CH_3); mass spectra: calculated for $C_{18}H_{18}N_4O$ = 306.1481; observed = 307.1638 $[M + H]^+$.

3-(5-(3-Methoxyphenyl)-4,5-dihydro-1H-pyrazol-3-yl)-2,6-dimethylimidazo[1,2-a]pyridine (2n). White solid; MP: 106−108 °C; yield: 77%; ^{1}H NMR (500 MHz, $CDCl_3$): δ 9.32 (s, 1H, Ar−H), 7.47 (d, J = 9.0 Hz, 1H, Ar−H), 7.28 (d, J = 8.0 Hz, 1H, Ar−H), 7.12 (dd, J = 9.1, 1.0 Hz, 1H, Ar−H), 6.98 (d, J = 7.4 Hz, 2H, Ar−H), 6.84 (dd, J = 7.5, 1.9 Hz, 1H, Ar−H), 5.96 (s, 1H, NH), 4.87 (t, J = 9.6 Hz, 1H, CH), 3.80 (s, 3H, OCH_3), 3.68 (dd, J = 15.9, 10.5 Hz, 1H, CH_2), 3.24 (dd, J = 15.8, 8.8 Hz, 1H, CH_2), 2.58 (s, 3H, CH_3), 2.37 (s, 3H, CH_3); ^{13}C NMR (100 MHz, $CDCl_3$) δ 160.09, 145.05, 145.01, 144.91, 144.23, 130.07, 128.75, 126.38, 122.58, 118.76, 115.61, 114.83, 113.24, 112.07, 63.26 (CH), 55.37 (OCH_3), 44.34 (CH_2), 18.56 (CH_3), 16.24 (CH_3); mass spectra: calculated for $C_{19}H_{20}N_4O$ = 320.1637; observed = 321.1789 $[M + H]^+$.

(3-(2,6-Dimethylimidazo[1,2-a]pyridin-3-yl)-5-(3,4,5-trimethoxyphenyl)-4,5-dihydro-1H-pyrazol-1-yl)(3-fluorophenyl)methanone (3a). Brown solid; MP: 176−178 °C; yield: 92%; ^{1}H NMR (400 MHz, $CDCl_3$) δ 9.09 (s, 1H, Ar−H), 7.77 (t, J = 9.0 Hz, 2H, Ar−H), 7.63 (d, J = 8.8 Hz, 1H, Ar−H), 7.47 (dt, J = 22.0, 6.9 Hz, 2H, Ar−H), 7.24 (s, 1H, Ar−H), 6.58 (s, 2H, Ar−H), 5.72 (dd, J = 11.6, 5.0 Hz, 1H, CH), 4.02 (dd, J = 17.2, 11.7 Hz, 1H, CH_2), 3.86 (s, 6H, OCH_3), 3.84 (s, 3H, OCH_3), 3.47 (dd, J = 17.2, 5.1 Hz, 1H, CH_2), 2.66 (s, 3H, CH_3), 2.31 (s, 3H, CH_3); ^{13}C NMR (100 MHz, $CDCl_3$) δ 165.13, 163.08, 161.13, 160.20, 147.94, 147.64, 145.30, 143.02, 137.24, 137.18, 130.38, 130.33, 129.58, 129.52, 126.77, 125.32, 117.88, 117.70, 116.71 (CH), 116.71, 116.52, 115.69, 113.57. 112.99, 111.90, 59.48, 59.48 (CH), 55.36 (OCH_3), 44.32 (OCH_3), 18.28 (CH_3), 16.23 (CH_3); mass spectra: calculated for $C_{28}H_{27}FN_4O_4$ = 502.2016; observed = 503.2769 $[M + H]^+$.

(5-(4-Chlorophenyl)-3-(2,6-dimethylimidazo[1,2-a]-pyridin-3-yl)-4,5-dihydro-1H-pyrazol-1-yl)(3-fluorophenyl)-methanone (3b). White solid; MP: 115−120 °C; yield: 91%; ^{1}H NMR (400 MHz, $CDCl_3$): δ 9.12 (s, 1H, Ar−H), 7.92 (d, J = 7.2 Hz, 1H, Ar−H), 7.86−7.69 (m, 4H, Ar−H), 7.47 (s, 2H, Ar−H), 7.35 (d, J = 6.7 Hz, 3H, Ar−H), 5.78 (d, J = 7.6 Hz, 1H, CH), 4.10−3.97 (m, 1H, CH_2), 3.43 (d, J = 14.3 Hz, 1H, CH_2), 2.68 (s, 3H, CH_3), 2.32 (s, 3H, CH_3); ^{13}C NMR (100 MHz, $CDCl_3$) δ 165.70, 145.87, 143.57, 135.78, 133.65, 133.22, 131.76, 130.06, 129.65, 129.07, 128.39, 127.19, 126.84, 126.74, 126.52, 125.79, 123.20, 114.30, 112.46, 56.03, 44.78, 17.32, 14.74; mass spectra: calculated for $C_{25}H_{20}ClFN_4O$ = 446.1300; observed = 447.1939 $[M + H]^+$.

(5-(4-Bromophenyl)-3-(2,6-dimethylimidazo[1,2-a]-pyridin-3-yl)-4,5-dihydro-1H-pyrazol-1-yl)(3-fluorophenyl)-methanone (3c). White solid; MP: 146−148 °C; yield: 94%; ^{1}H NMR (400 MHz, $CDCl_3$) δ 9.09 (s, 1H, Ar−H), 7.91 (s, 1H, Ar−H), 7.84−7.66 (m, 4H, Ar−H), 7.52 (d, J = 8.0 Hz, 2H, Ar−H), 7.26 (s, 3H, Ar−H), 5.76 (d, J = 7.1 Hz, 1H, CH), 4.03 (d, J = 5.1 Hz, 1H, CH_2), 3.43 (dd, J = 17.1, 4.2 Hz, 1H, CH_2), 2.67 (s, 3H, CH_3), 2.31 (s, 3H, CH_3); ^{13}C NMR (100 MHz, $CDCl_3$) δ 163.23, 161.32, 160.78, 147.34, 140.24, 136.82, 132.25, 130.65, 129.78, 129.53, 129.45, 127.56, 126.58, 125.19, 124.32, 121.96, 119.83, 119.63, 117.95, 117.74, 116.62, 116.39, 115.54, 59.06, 43.96, 18.16, 15.74; mass spectra: calculated for $C_{25}H_{20}BrFN_4O$ = 491.3500; observed = 493.1526 $[M + H]^+$.

(3-(2,6-Dimethylimidazo[1,2-a]pyridin-3-yl)-5-(4-fluorophenyl)-4,5-dihydro-1H-pyrazol-1-yl)(3-fluorophenyl)-methanone (3d). Brown solid; MP: 116−118 °C; yield: 97%; ^{1}H NMR (400 MHz, $CDCl_3$): δ 9.09 (s, 1H, Ar−H), 7.91 (s, 1H, Ar−H), 7.75 (s, 4H, Ar−H), 7.44 (d, J = 15.6 Hz, 2H, Ar−H), 7.37 (s, 3H, Ar−H), 5.79 (d, J = 5.6 Hz, 1H, CH), 4.07−4.00 (m, 1H, CH_2), 3.44 (d, J = 14.8 Hz, 1H, CH_2), 2.68 (s, 3H, CH_3), 2.30 (s, 3H, CH_3); ^{13}C NMR (100 MHz, $CDCl_3$) δ 163.76, 163.57, 163.22, 161.31, 161.12, 147.37, 137.02, 136.85, 130.70, 129.85, 129.77, 129.52, 129.44, 127.62, 127.54, 126.58, 125.65, 125.16, 124.36, 119.85, 119.63, 117.90, 117.69, 116.60, 116.37, 116.12, 115.90, 115.47, 77.31, 76.99, 76.67, 58.91, 44.10, 18.15, 15.60; mass spectra: calculated for $C_{25}H_{20}F_2N_4O$ = 430.1605; observed = 431.2112 $[M + H]^+$.

(3-(2,6-Dimethylimidazo[1,2-a]pyridin-3-yl)-5-(4-fluorophenyl)-4,5-dihydro-1H-pyrazol-1-yl)(phenyl)methanone (3e). White solid; MP: 132−134 °C; yield = 90%; ^{1}H NMR (400 MHz, DMSO-d_6): δ 8.95 (s, 1H, Ar−H), 7.88 (d, J = 7.0 Hz, 2H, Ar−H), 7.61−7.51 (m, 4H, Ar−H), 7.49−7.43 (m, 2H, Ar−H), 7.28 (d, J = 8.9 Hz, 1H, Ar−H), 7.20 (t, J = 8.7 Hz, 2H, Ar−H), 5.74 (dd, J = 11.6, 4.9 Hz, 1H, CH), 4.16 (dd, J = 17.4, 11.8 Hz, 1H, CH_2), 3.39−3.34 (m, 1H, CH_2), 2.51 (s, 3H, CH_3), 2.20 (s, 3H, CH_3); ^{13}C NMR (100 MHz, DMSO-d_6) δ 166.07, 163.09, 160.68, 148.69, 147.96, 145.07, 138.86, 135.82, 131.07, 129.88, 129.31, 128.32, 126.27, 123.38, 115.84, 113.41, 58.67, 44.16, 18.30, 16.34; mass spectra: calculated for $C_{25}H_{21}FN_4O$ = 412.1669; observed = 413.1519 $[M + H]^+$.

(3-(2,6-Dimethylimidazo[1,2-a]pyridin-3-yl)-5-(4-fluorophenyl)-4,5-dihydro-1H-pyrazol-1-yl)(3-methoxyphenyl)-methanone (3f). Yellow solid; MP: 126−128 °C; yield = 96%; ^{1}H NMR (400 MHz, DMSO-d_6): δ 8.99 (s, 1H, Ar−H), 7.61−7.17 (m, 9H, Ar−H), 5.74 (s, 1H, CH), 4.16 (s, 1H, CH_2), 3.82 (s, 3H, OCH_3), 3.39 (s, 1H, CH_2), 2.53 (s, 3H, CH_3), 2.21 (s, 3H, CH_3); ^{13}C NMR (100 MHz, DMSO-d_6) δ 166.74, 163.10, 160.69, 148.24, 147.92, 144.83, 138.80, 137.80, 130.18, 129.54, 128.43, 126.34, 123.63, 121.53, 116.399, 115.83, 114.92, 113.51, 58.80 (CH), 55.67 (OCH_3), 44.16 (CH_2), 18.30 (CH_3), 16.34 (CH_3); mass spectra: calculated for $C_{26}H_{23}FN_4O_2$ = 442.1805; observed = 443.2291 $[M + H]^+$.

(3-(2,6-Dimethylimidazo[1,2-a]pyridin-3-yl)-5-(4-fluorophenyl)-4,5-dihydro-1H-pyrazol-1-yl)(4-methoxyphenyl)-methanone (3g). Yellow solid; MP: 102−104 °C; Yield = 96%; ^{1}H NMR (400 MHz, DMSO-d_6): δ 9.07 (s, 1H, Ar−H), 7.92 (d, J = 7.8 Hz, 2H, Ar−H), 7.56 (d, J = 8.7 Hz, 1H, Ar−H), 7.43 (s, 2H, Ar−H), 7.32 (d, J = 8.6 Hz, 1H, Ar−H), 7.20 (d, J = 7.9 Hz, 2H, Ar−H), 7.09 (d, J = 7.7 Hz, 2H, Ar−H), 5.72 (d, J = 7.2 Hz, 1H, CH), 4.22−4.09 (m, 1H, CH_2), 3.85 (s, 3H, OCH_3), 2.51 (d, J = 5.1 Hz, 3H, CH_3), 2.27 (s, 3H, CH_3); ^{13}C NMR (100 MHz, DMSO-d_6) δ 165.56, 161.63, 148.60, 147.67, 145.06, 139.05, 131.56, 129.88, 128.51, 128.42, 127.62, 126.31, 123.40, 116.04, 116.01, 115.80, 113.53, 58.78 (CH), 55.86 (OCH_3), 44.03 (CH_2), 18.34 (CH_3), 16.37 (CH_3); mass spectra: calculated for $C_{26}H_{23}FN_4O_2$ = 442.1805; observed = 443.2205 $[M + H]^+$.

(3-(2,6-Dimethylimidazo[1,2-a]pyridin-3-yl)-5-(4-fluorophenyl)-4,5-dihydro-1H-pyrazol-1-yl)(3,5-dinitrophenyl)-methanone (3h). Yellow solid; MP: 124−126 °C; Yield = 96%; 1H NMR^{1}H NMR (400 MHz, DMSO-d_6): δ 9.05 (d, J = 15.1 Hz, 3H, Ar−H), 8.78 (s, 1H, Ar−H), 7.59−7.50 (m, 3H, Ar−H), 7.30 (d, J = 8.9 Hz, 1H, Ar−H), 7.21 (t, J = 8.6 Hz, 2H, Ar−H), 5.78 (dd, J = 11.2, 4.7 Hz, 1H, CH), 4.24 (dd, J = 17.3, 11.6 Hz, 1H, CH_2), 3.47 (d, J = 4.8 Hz, 1H, CH_2), 2.55 (s, 3H, CH_3), 2.02 (s, 3H, CH_3); ^{13}C NMR (100 MHz, DMSO-d_6) δ 161.40, 160.82, 160.80, 150.15, 148.24, 138.19, 137.99, 130.38, 129.81, 128.84, 128.76, 125.89, 123.73, 120.93,

https://doi.org/10.1021/acsomega.3c10504
ACS Omega 2025, 10, 114−126

116.22, 116.06, 115.85, 59.27, 44.56, 18.10, 16.66; mass spectra: calculated for $C_{25}H_{19}FN_6O_5$ = 502.1401; observed = 503.1851 $[M + H]^+$.

(3-(2,6-Dimethylimidazo[1,2-a]pyridin-3-yl)-5-(4-fluorophenyl)-4,5-dihydro-1H-pyrazol-1-yl)(2-fluorophenyl)-methanone (3i). Orange solid; MP: 132−134 °C; yield = 95%; ^{1}H NMR (400 MHz, DMSO-d_6): δ 8.69 (s, 1H, Ar−H), 7.87 (t, J = 7.6 Hz, 1H, Ar−H), 7.61−7.56 (m, 1H, Ar−H), 7.53 (d, J = 9.0 Hz, 1H, Ar−H), 7.45 (s, 1H, Ar−H), 7.42 (d, J = 5.2 Hz, 1H, Ar−H), 7.37 (d, J = 7.5 Hz, 1H, Ar−H), 7.28 (d, J = 4.7 Hz, 1H, Ar−H), 7.23 (t, J = 8.8 Hz, 2H, Ar−H), 5.74 (dd, J = 11.6, 4.7 Hz, 1H, CH), 4.23 (dd, J = 17.5, 11.7 Hz, 1H, CH_2), 3.43−3.37 (m, 1H, CH_2), 2.50 (s, 3H, CH_3), 2.13 (s, 3H); ^{13}C NMR (100 MHz, DMSO-d_6) δ 165.48, 163.17, 162.55, 160.75, 157.52, 148.84, 148.46, 145.12, 138.31, 135.20, 135.11, 132.43, 132.35, 130.01, 129.88, 128.43, 128.35, 125.94, 125.45, 125.28, 125.05, 124.93, 123.49, 117.49, 117.27, 116.13, 116.04, 115.98, 115.92, 113.26, 58.37, 44.74, 18.28, 16.22; mass spectra: calculated for $C_{25}H_{21}FN_4O$ = 430.1605; observed = 431.2112 $[M + H]^+$.

(5-(3,4-Dimethoxyphenyl)-3-(2,6-dimethylimidazo[1,2-a]-pyridin-3-yl)-4,5-dihydro-1H-pyrazol-1-yl)(3-fluorophenyl)-methanone (3j). Yellow solid; MP: 98−100 °C; yield: 97%; ^{1}H NMR (500 MHz, $CDCl_3$): δ 9.05 (s, 1H, Ar−H), 7.79−7.65 (m, 2H, Ar−H), 7.53 (d, J = 9.0 Hz, 1H, Ar−H), 7.51−7.37 (m, 1H, Ar−H), 7.30−7.14 (m, 2H, Ar−H), 6.89 (s, 2H, Ar−H), 6.83 (d, J = 8.0 Hz, 1H, Ar−H), 5.71 (dd, J = 11.5, 4.7 Hz, 1H, CH), 3.98 (dd, J = 17.0, 11.5 Hz, 1H, CH_2), 3.86 (s, 3H, OCH_3), 3.84 (s, 3H, OCH_3), 3.44 (dd, J = 17.0, 4.9 Hz, 1H, CH_2), 2.61 (s, 3H, CH_3), 2.26 (s, 3H, CH_3); ^{13}C NMR (100 MHz, $CDCl_3$) δ 165.17, 165.17, 163.08, 161.12, 149.44, 148.85, 148.19, 147.75, 145.47, 137.33, 137.27, 134.05, 130.18, 129.59, 129.53, 126.72, 125.27, 123.93, 117.84, 117.78, 117.68, 116.67, 116.49, 115.78, 111.75, 109.46, 59.37 (CH), 56.08 (OCH_3), 56.03 (OCH_3), 44.35 (CH_2), 18.28 (CH_3), 16.33 (CH_3); mass spectra: calculated for $C_{27}H_{25}FN_4O_3$ = 472.1911; observed = 473.2660 $[M + H]^+$.

(5-(3,4-Dimethoxyphenyl)-3-(2,6-dimethylimidazo[1,2-a]-pyridin-3-yl)-4,5-dihydro-1H-Pyrazol-1-yl)(phenyl)-methanone (3k). Yellow solid; MP: 110−112 °C; yield = 92%; ^{1}H NMR (400 MHz, $CDCl_3$): δ 9.02 (s, 1H, Ar−H), 8.03 (d, J = 5.7 Hz, 1H, Ar−H), 7.89 (s, 2H, Ar−H), 7.50 (s, 2H, Ar−H), 7.43 (d, J = 6.6 Hz, 1H, Ar−H), 7.14 (d, J = 8.4 Hz, 1H), 6.85 (s, 2H, Ar−H), 6.79 (s, 1H, Ar−H), 5.67 (d, J = 7.4 Hz, 1H, CH), 3.90 (d, J = 12.5 Hz, 1H, CH_2), 3.81 (s, 3H, OCH_3), 3.79 (s, 3H, OCH_3), 3.38 (d, J = 16.8 Hz, 1H, CH_2), 2.56 (s, 3H, CH_3), 2.18 (s, 3H, CH_3); ^{13}C NMR (100 MHz, $CDCl_3$) δ 165.76, 148.30, 147.65, 146.42, 146.04, 144.06, 134.24, 133.16, 129.71, 128.83, 128.26, 126.74, 125.72, 122.73, 116.68, 114.49, 112.61, 110.64, 108.32, 58.19 (CH), 54.96 (OCH_3), 54.93 (OCH_3), 44.80 (CH_2), 17.30 (CH_3), 14.94 (CH_3); mass spectra: calculated for $C_{27}H_{26}N_4O_3$ = 454.2005; observed = 455.2375 $[M + H]^+$.

(5-(3,4-Dimethoxyphenyl)-3-(2,6-dimethylimidazo[1,2-a]-pyridin-3-yl)-4,5-dihydro-1H-pyrazol-1-yl)(3,5-dinitrophenyl)methanone (3l). Brown solid; MP: 114−116 °C; yield = 88%; ^{1}H NMR (400 MHz, $CDCl_3$): δ 9.16 (s, 2H, Ar−H), 8.76 (s, 1H, Ar−H), 7.47 (s, 1H, Ar−H), 7.19 (s, 2H, Ar−H), 6.84 (d, J = 19.8 Hz, 3H, Ar−H), 5.68 (s, 1H, CH), 4.02 (d, J = 18.1 Hz, 1H, CH_2), 3.84 (s, 3H, OCH_3), 3.80 (s, 3H, OCH_3), 3.49 (d, J = 18.0 Hz, 1H, CH_2), 2.59 (s, 3H, CH_3), 2.03 (s, 3H, CH_3); ^{13}C NMR (100 MHz, $CDCl_3$) δ 159.96, 148.90, 148.77, 148.07, 147.05, 144.93, 137.48, 132.00, 129.44, 128.82, 128.43, 124.93, 123.01, 119.31, 116.83, 115.12, 111.99, 110.68, 108.63, 58.67 (CH), 55.07 (OCH_3), 54.94 (OCH_3), 44.73 (CH_2), 17.35 (CH_3), 15.77 (CH_3); mass spectra: calculated for $C_{27}H_{24}N_6O_7$ = 544.1706; observed = 545.2237 $[M + H]^+$.

(5-(3,4-Dimethoxyphenyl)-3-(2,6-dimethylimidazo[1,2-a]-pyridin-3-yl)-4,5-dihydro-1H-pyrazol-1-yl)(3-methoxyphenyl)methanone (3m). Yellow solid; MP: 109−111 °C; yield = 86%; ^{1}H NMR (400 MHz, $CDCl_3$): δ 9.13 (s, 1H, Ar−H), 7.53 (d, J = 21.5 Hz, 3H, Ar−H), 7.40 (s, 1H, Ar−H), 7.21 (s, 1H, Ar−H), 7.08 (s, 1H, Ar−H), 6.92 (s, 2H, Ar−H), 5.73 (s, 1H, CH), 3.97 (d, J = 15.6 Hz, 1H, CH_2), 3.85 (s, 9H, $(OCH_3)_3$), 3.45 (d, J = 17.2 Hz, 1H, CH_2), 2.62 (s, 3H, CH_3), 2.27 (s, 3H, CH_3); ^{13}C NMR (100 MHz, $CDCl_3$) δ 165.47, 158.07, 148.33, 147.72, 145.57, 144.50, 142.79, 135.32, 132.95, 130.26, 127.80, 125.99, 123.78, 120.59, 116.64, 115.48, 113.88, 113.68, 112.86, 110.66, 108.30, 58.37 (CH), 54.98 (OCH_3), 54.94 (OCH_3), 54.31 (OCH_3), 44.83 (CH_2), 17.17 (CH_3), 14.31 (CH_3); mass spectra: calculated for $C_{28}H_{28}N_4O_4$ = 484.2111; observed = 485.2244 $[M + H]^+$.

(5-(3,4-Dimethoxyphenyl)-3-(2,6-dimethylimidazo[1,2-a]-pyridin-3-yl)-4,5-dihydro-1H-pyrazol-1-yl)(4-methoxyphenyl)methanone (3n). Orange solid; MP: 142−144 °C; yield = 92%; ^{1}H NMR (400 MHz, $CDCl_3$): δ 9.19 (s, 1H, Ar−H), 8.04 (s, 2H, Ar−H), 7.55 (d, J = 7.7 Hz, 1H, Ar−H), 7.21 (d, J = 7.3 Hz, 1H, Ar−H), 6.99 (d, J = 6.4 Hz, 2H, Ar−H), 6.91 (s, 2H, Ar−H), 6.86 (s, 1H, Ar−H), 5.74 (d, J = 7.2 Hz, 1H, CH), 3.96 (d, J = 12.3 Hz, 1H, CH_2), 3.88 (s, 6H, $(OCH_3)_2$), 3.85 (s, 3H, OCH_3), 3.43 (d, J = 17.3 Hz, 1H, CH_2), 2.63 (s, 3H, CH_3), 2.32 (s, 3H, CH_3); ^{13}C NMR (100 MHz, $CDCl_3$) δ 164.23, 156.83, 147.09, 146.48, 144.33, 141.55, 134.08, 131.71, 129.02, 126.56, 124.75, 122.54, 119.35, 115.40, 114.24, 112.44, 111.62, 109.42, 107.06, 57.13 (CH), 53.74 (OCH_3), 53.07 (OCH_3), 43.58 (CH_2), 15.93 (CH_3), 13.07 (CH_3); mass spectra: calculated for $C_{28}H_{28}N_4O_4$ = 484.2111; observed = 485.2517 $[M + H]^+$.

(5-(2,4-Dichlorophenyl)-3-(2,6-dimethylimidazo[1,2-a]-pyridin-3-yl)-4,5-dihydro-1H-pyrazol-1-yl)(3-fluorophenyl)-methanone (3o). Yellow solid; MP: 138−140 °C; yield: 97%; ^{1}H NMR (500 MHz, $CDCl_3$): δ 9.06 (s, 1H, Ar−H), 7.81−7.76 (m, 2H, Ar−H), 7.54 (d, J = 9.0 Hz, 1H, Ar−H), 7.50−7.45 (m, 2H, Ar−H), 7.28−7.25 (m, 1H, Ar−H), 7.24−7.19 (m, 3H, Ar−H), 6.03 (dd, J = 11.8, 5.4 Hz, 1H, CH), 4.06 (dd, J = 17.2, 11.8 Hz, 1H, CH_2), 3.31 (dd, J = 17.2, 5.4 Hz, 1H, CH_2), 2.60 (s, 3H, CH_3), 2.28 (s, 3H, CH_3); ^{13}C NMR (100 MHz, $CDCl_3$) δ 165.14, 163.12, 161.16, 148.42, 147.82, 145.56, 136.78, 134.41, 132.89, 130.33, 130.21, 129.87, 129.71, 129.64, 127.89, 127.55, 126.71, 125.43, 124.06, 118.19, 118.02, 118.02, 116.81, 116.62, 115.85, 77.37, 77.11, 76.86, 57.15, 42.92, 18.30, 16.38; mass spectra: calculated for $C_{25}H_{19}Cl_2FN_4O$ = 480.0920; observed = 481.1536 $[M + H]^+$.

(5-(2,4-Dichlorophenyl)-3-(2,6-dimethylimidazo[1,2-a]-pyridin-3-yl)-4,5-dihydro-1H-pyrazol-1-yl)(phenyl)-methanone (3p). Yellow solid; MP: 150−152 °C; yield = 95%; ^{1}H NMR (400 MHz, DMSO) δ 8.94 (s, 1H, Ar−H), 7.93 (d, J = 7.0 Hz, 2H, Ar−H), 7.70 (s, 1H, Ar−H), 7.67−7.50 (m, 4H, Ar−H), 7.41 (q, J = 8.3 Hz, 2H, Ar−H), 7.28 (d, J = 8.9 Hz, 1H, Ar−H), 5.92 (dd, J = 11.6, 5.2 Hz, 1H, CH), 4.19 (dd, J = 17.1, 12.2 Hz, 1H, CH_2), 2.50 (s, 3H, CH_3), 2.20 (s, 3H, CH_3); ^{13}C NMR (100 MHz, DMSO-d_6) δ 166.03, 148.91, 148.11, 145.14, 138.45, 135.42, 133.17, 132.66, 131.26, 129.93, 129.71, 129.62, 129.41, 128.42, 128.35, 126.25, 123.44, 116.01, 113.23, 56.77, 42.57, 18.31, 16.33; mass spectra:

https://doi.org/10.1021/acsomega.3c10504
ACS Omega 2025, 10, 114−126

calculated for $C_{25}H_{20}Cl_2N_4O$ = 462.1014; observed = 463.1502 $[M + H]^+$.

(5-(2,4-Dichlorophenyl)-3-(2,6-dimethylimidazo[1,2-a]-pyridin-3-yl)-4,5-dihydro-1H-pyrazol-1-yl)(3,5-dinitrophenyl)methanone (3q). White solid; MP: 102−104 °C; yield = 96%; ^{1}H NMR (400 MHz, $CDCl_3$) δ 9.28 (s, 2H, Ar−H), 9.23−9.18 (m, 2H, Ar−H), 8.83 (s, 1H, Ar−H), 7.52 (s, 2H, Ar−H), 7.24 (s, 1H, Ar−H), 6.08 (s, 1H, Ar−H), 4.11 (d, J = 33.3 Hz, 1H, CH), 3.43 (d, J = 16.8 Hz, 1H, CH_2), 2.64 (s, 3H, CH_3), 2.12 (s, 3H, CH_3); ^{13}C NMR (100 MHz, $CDCl_3$) δ 160.02, 148.70, 148.07, 147.39, 147.14, 144.45, 136.83, 134.75, 133.80, 131.86, 129.31, 128.87, 128.44, 126.98, 126.63, 124.94, 119.63, 114.88, 111.84, 56.47, 44.78, 17.38, 15.32; mass spectra: calculated for $C_{25}H_{18}Cl_2N_6O_5$ = 552.0716; observed = 553.1284 $[M + H]^+$.

(5-(2,4-Dichlorophenyl)-3-(2,6-dimethylimidazo[1,2-a]-pyridin-3-yl)-4,5-dihydro-1H-Pyrazol-1-yl)(3-methoxyphenyl)methanone (3r). Yellow solid; MP: 120−122 °C; yield = 92%; ^{1}H NMR (400 MHz, $CDCl_3$): δ 9.12 (s, 1H, Ar−H), 7.64 (s, 1H, Ar−H), 7.59−7.46 (m, 3H, Ar−H), 7.43 (s, 1H, Ar−H), 7.26 (s, 1H, Ar−H), 7.23 (s, 2H, Ar−H), 7.11 (s, 1H, Ar−H), 6.06 (s, 1H, CH), 4.15−4.00 (m, 1H, CH_2), 3.86 (s, 3H, CH_3), 3.33−3.29 (m, 1H, CH_2), 2.61 (s, 3H, CH_3), 2.28 (s, 3H, CH_3); ^{13}C NMR (100 MHz, $CDCl_3$) δ 165.26, 158.08, 147.34, 146.31, 144.57, 135.95, 134.87, 133.13, 131.75, 129.01, 128.86, 127.80, 126.74, 126.41, 125.74, 122.60, 120.83, 115.77, 114.74, 113.79, 112.33, 55.97 (CH), 54.31 (OCH_3), 44.82 (CH_2), 17.17 (CH_3), 15.34 (CH_3); mass spectra: calculated for $C_{26}H_{22}Cl_2N_4O_2$ = 492.1120; observed = 493.0882 $[M + H]^+$.

(5-(2,4-Dichlorophenyl)-3-(2,6-dimethylimidazo[1,2-a]-pyridin-3-yl)-4,5-dihydro-1H-pyrazol-1-yl)(2-fluorophenyl)-methanone (3s). White solid; MP: 140−142 °C; yield = 90%; ^{1}H NMR (400 MHz, $CDCl_3$): δ 8.82 (s, 1H, Ar−H), 7.63 (s, 1H, Ar−H), 7.49 (s, 3H, Ar−H), 7.32−7.24 (m, 4H, Ar−H), 7.17 (s, 1H, Ar−H), 6.05 (s, 1H, CH), 4.12−4.10 (m, 1H, CH_2), 3.32−3.28 (m, 1H, CH_2), 2.58 (s, 3H, CH_3), 2.19 (s, 3H, CH_3); ^{13}C NMR (100 MHz, $CDCl_3$) δ 162.42, 159.25, 156.77, 145.40, 134.98, 133.55, 131.69, 131.24, 131.16, 129.09, 129.00, 126.95, 126.33, 126.01, 124.85, 123.57, 123.30, 114.60, 114.39, 113.17, 112.71, 55.65, 44.81, 17.35, 13.32; mass spectra: calculated for $C_{25}H_{19}Cl_2FN_4O$ = 480.0920; observed = 481.1446 $[M + H]^+$.

(5-(2,4-Dichlorophenyl)-3-(2,6-dimethylimidazo[1,2-a]-pyridin-3-yl)-4,5-dihydro-1H-pyrazol-1-yl)(4-methoxyphenyl)methanone (3t). Yellow solid; MP: 110−112 °C; yield = 92%; ^{1}H NMR (400 MHz, $CDCl_3$): δ 9.18 (s, 1H, Ar−H), 8.09 (s, 3H, Ar−H), 7.54 (s, 1H, Ar−H), 7.47 (s, 1H, Ar−H), 7.27 (s, 1H, Ar−H), 7.00 (s, 3H, Ar−H), 6.05 (s, 1H, CH), 4.05 (t, J = 13.4 Hz, 1H, CH_2), 3.90 (s, 3H, OCH_3), 3.30 (d, J = 17.6 Hz, 1H, CH_2), 2.61 (s, 3H, CH_3), 2.33 (s, 3H, CH_3); ^{13}C NMR (100 MHz, $CDCl_3$) δ 165.00, 163.55, 161.27, 160.88, 147.13, 146.00, 136.16, 133.04, 131.80, 130.70, 128.97, 128.78, 126.69, 125.63, 122.45, 120.21, 114.77, 113.11, 112.01, 56.10 (CH), 54.41 (OCH_3), 44.59 (CH_2), 17.40 (CH_3), 15.27 (CH_3); mass spectra: calculated for $C_{26}H_{22}Cl_2N_4O_2$ = 492.1120; observed = 493.1617 $[M + H]^+$.

(3-(2,6-Dimethylimidazo[1,2-a]pyridin-3-yl)-5-(4-nitro-phenyl)-1H-pyrazol-1-yl)(3-fluorophenyl)methanone (3u). White solid; MP: 198−200 °C; yield: 97%; ^{1}H NMR (400 MHz, $CDCl_3$): δ 9.08 (s, 1H, Ar−H), 8.25 (d, J = 8.7 Hz, 2H, Ar−H), 7.77 (d, J = 8.2 Hz, 2H, Ar−H), 7.55 (dd, J = 8.7, 4.8 Hz, 3H, Ar−H), 7.47 (dd, J = 7.9, 5.7 Hz, 1H, Ar−H), 7.24 (d, J = 9.1 Hz, 2H, Ar−H), 5.85 (dd, J = 11.7, 5.2 Hz, 1H, CH), 4.09 (dd, J = 17.2, 11.8 Hz, 1H, CH_2), 3.42 (dd, J = 17.2, 5.2 Hz, 1H, CH_2), 2.61 (s, 3H, CH_3), 2.30 (s, 3H, CH_3); ^{13}C NMR (100 MHz, $CDCl_3$) δ 149.73, 147.67, 144.71, 132.84, 129.22, 128.78, 128.58, 127.60, 127.40, 127.35, 126.68, 126.35, 126.29, 124.51, 124.39, 124.27, 123.98, 122.99, 116.02, 115.60, 77.35, 77.10, 76.84, 62.71, 44.52, 18.58, 16.14; mass spectra: calculated for $C_{25}H_{18}FN_5O_3$ = 455.1394; observed = 456.2601 $[M + H]^+$.

(3-(2,6-Dimethylimidazo[1,2-a]pyridin-3-yl)-5-(4-nitro-phenyl)-4,5-dihydro-1H-pyrazol-1-yl)(phenyl)methanone (3v). White solid; MP: 128−130 °C; yield = 90%; ^{1}H NMR (400 MHz, $CDCl_3$): δ 9.07 (s, 1H, Ar−H), 8.23 (d, J = 8.6 Hz, 2H, Ar−H), 7.98 (d, J = 7.1 Hz, 2H, Ar−H), 7.60−7.46 (m, 6H, Ar−H), 7.23−7.16 (m, 1H, Ar−H), 5.85 (dd, J = 11.7, 5.3 Hz, 1H, CH), 4.11−4.02 (m, 1H, CH_2), 3.40 (dd, J = 17.2, 5.3 Hz, 1H, CH_2), 2.60 (s, 3H, CH_3), 2.26 (s, 3H, CH_3); ^{13}C NMR (100 MHz, DMSO-d_6) δ 166.13, 149.95, 148.87, 147.98, 147.27, 145.12, 135.45, 131.25, 129.95, 129.40, 128.34, 127.83, 126.25, 124.48, 123.44, 115.97, 113.25, 46.02, 43.75, 18.28, 16.33; mass spectra: calculated for $C_{25}H_{21}N_5O_3$ = 439.1644; observed = 440.1452 $[M + H]^+$.

(3-(2,6-Dimethylimidazo[1,2-a]pyridin-3-yl)-5-(4-nitro-phenyl)-4,5-dihydro-1H-pyrazol-1-yl)(2-fluorophenyl)-methanone (3w). Yellow solid; MP: 144−146 °C; yield = 95%; ^{1}H NMR (400 MHz, $CDCl_3$): δ 8.86 (s, 1H, Ar−H), 8.27 (d, J = 8.6 Hz, 2H, Ar−H), 7.67−7.48 (m, 6H, Ar−H), 7.31 (d, J = 7.5 Hz, 1H, Ar−H), 7.22 (d, J = 9.2 Hz, 1H, Ar−H), 5.86 (dd, J = 11.8, 5.0 Hz, 1H, CH), 4.13 (dd, J = 17.1, 11.9 Hz, 1H, CH_2), 3.41 (dd, J = 17.2, 5.0 Hz, 1H, CH_2), 2.63 (s, 3H, CH_3), 2.21 (s, 3H, CH_3); ^{13}C NMR (100 MHz, $CDCl_3$) δ 166.67, 148.57, 148.36, 147.52, 146.78, 145.64, 134.52, 131.08, 129.93, 129.37, 127.80, 126.84, 126.66, 124.42, 123.61, 115.81, 113.20, 77.33, 77.01, 76.70, 59.00, 43.80, 18.30, 16.36; mass spectra: calculated for $C_{25}H_{20}FN_5O_3$ = 457.1550; observed = 458.1274 $[M + H]^+$.

(2,6-Difluorophenyl)(3-(2,6-dimethylimidazo[1,2-a]-pyridin-3-yl)-5-(4-nitrophenyl)-4,5-dihydro-1H-pyrazol-1-yl)-methanone (3x). Yellow solid; MP: 126−128 °C; yield = 90%; ^{1}H NMR (400 MHz, $CDCl_3$): δ 8.74 (s, 1H, Ar−H), 8.27 (d, J = 8.6 Hz, 2H, Ar−H), 7.65 (d, J = 9.0 Hz, 1H, Ar−H), 7.57 (d, J = 8.6 Hz, 2H, Ar−H), 7.54−7.44 (m, 1H, Ar−H), 7.28 (d, J = 9.1 Hz, 1H, Ar−H), 7.06 (d, J = 8.6 Hz, 2H, Ar−H), 5.88 (dd, J = 11.7, 4.7 Hz, 1H, CH), 4.23−4.11 (m, 1H, CH_2), 3.42 (dd, J = 17.2, 4.8 Hz, 1H, CH_2), 2.63 (s, 3H, CH_3), 2.17 (s, 3H, CH_3); ^{13}C NMR (101 MHz, cdcl$_3$) δ 173.18, 149.96, 148.64, 147.58, 146.05, 143.87, 138.53, 132.10, 129.86, 128.73, 125.92, 125.55, 123.73, 122.69, 120.75, 116.29, 112.82, 61.22, 44.57, 18.81, 16.72.

(3-(2,6-Dimethylimidazo[1,2-a]pyridin-3-yl)-5-(thiophen-2-yl)-4,5-dihydro-1H-pyrazol-1-yl)(3-fluorophenyl)-methanone (3y). Brown solid; MP: 122−124 °C; yield: 93%; ^{1}H NMR (500 MHz, $CDCl_3$): δ 9.02 (s, 1H, Ar−H), 7.88 (d, J = 7.0 Hz, 1H, Ar−H), 7.82−7.63 (m, 3H, Ar−H), 7.64 (d, J = 7.1 Hz, 1H, Ar−H), 7.50−7.36 (m, 2H, Ar−H), 7.15 (s, 1H, Ar−H), 6.96 (s, 1H, Ar−H), 6.11 (d, J = 7.8 Hz, 1H, CH), 3.97 (dd, J = 16.5, 11.6 Hz, 1H, CH_2), 3.61 (d, J = 17.0 Hz, 1H, CH_2), 2.66 (s, 3H, CH_3), 2.26 (s, 3H, CH_3); 13C NMR (100 MHz, $CDCl_3$) δ 165.31, 163.08, 161.66, 147.63, 147.48, 145.13, 143.68, 137.03, 136.97, 133.68, 130.66, 129.96, 129.90, 129.61, 129.55, 127.12, 126.73, 125.66, 125.44, 125.30, 125.05, 124.31, 119.84, 119.67, 118.00, 117.83, 116.88, 116.70, 116.52, 115.59, 113.47, 55.00, 43.97, 18.28, 15.93; mass spectra:

https://doi.org/10.1021/acsomega.3c10504
ACS Omega 2025, 10, 114−126

calculated for $C_{23}H_{19}FN_4OS$ = 418.1300; observed = 419.1908 $[M + H]^+$.

(3-(2,6-Dimethylimidazo[1,2-a]pyridin-3-yl)-5-(3-fluorophenyl)-4,5-dihydro-1H-pyrazol-1-yl)(3-fluorophenyl)-methanone (3z). Yellow solid; MP: 126−128 °C; yield: 97%; ^{1}H NMR (400 MHz, $CDCl_3$): δ 9.10 (s, 1H, Ar−H), 7.90 (s, 1H, Ar−H), 7.75 (s, 4H, Ar−H), 7.46 (s, 2H, Ar−H), 7.42 (s, 1H, Ar−H), 7.37 (s, 2H, Ar−H), 5.80 (d, J = 5.6 Hz, 1H, CH), 4.07−4.00 (m, 1H, CH_2), 3.46−3.42 (m, 1H, CH_2), 2.68 (s, 3H, CH_3), 2.30 (s, 3H, CH_3); ^{13}C NMR (100 MHz, $CDCl_3$) δ 163.76, 163.57, 163.22, 161.31, 147.37, 137.01, 136.85, 130.69, 129.85, 129.77, 129.51, 129.43, 129.62, 127.63, 127.54, 126.58, 125.64, 125.16, 124.36, 119.84, 199.63, 117.90, 117.69, 116.60, 116.37, 116.12, 115.90, 115.47, 58.91, 44.10, 18.15, 15.60; mass spectra: calculated for $C_{25}H_{20}F_2N_4O$ = 430.1605; observed = 431.1404 $[M + H]^+$.

(3-(2,6-Dimethylimidazo[1,2-a]pyridin-3-Yl)-5-(4-methoxyphenyl)-4,5-dihydro-1H-pyrazol-1-Yl)(3-fluorophenyl)-methanone (3aa). Yellow solid; MP: 106−108 °C; yield: 97%; ^{1}H NMR (500 MHz, $CDCl_3$): δ 9.07 (s, 1H, Ar−H), 7.79−7.65 (m, 2H, Ar−H), 7.55 (d, J = 9.5 Hz, 1H, Ar−H), 7.51−7.36 (m, 1H, Ar−H), 7.29 (d, J = 8.5 Hz, 2H, Ar−H), 7.27−7.15 (m, 2H, Ar−H), 6.88 (d, J = 8.5 Hz, 2H, Ar−H), 5.72 (dd, J = 11.5, 5.0 Hz, 1H, CH), 3.98 (dd, J = 17.0, 11.5 Hz, 1H, CH_2), 3.77 (s, 3H, OCH_3), 3.43 (dd, J = 17.0, 4.5 Hz, 1H, CH_2), 2.61 (s, 3H, CH_3), 2.27 (s, 3H, CH_3); ^{13}C NMR (100 MHz, $CDCl_3$) δ 165.06, 163.07, 161.11, 159.38, 147.91, 147.66, 145.30, 137.36, 133.59, 130.29, 129.54, 129.48, 127.21, 126.75, 125.30, 124.02, 117.79, 117.63, 116.70, 116.52, 115.73, 114.54, 113.76, 113.63, 59.07 (CH), 55.40 (OCH_3), 44.27 (CH_2), 18.29 (CH_3), 16.26 (CH_3); mass spectra: calculated for $C_{26}H_{23}FN_4O_2$ = 442.1805; observed = 443.1560 $[M + H]^+$.

(3-(2,6-Dimethylimidazo[1,2-a]pyridin-3-yl)-5-(p-tolyl)-4,5-dihydro-1H-pyrazol-1-yl)(3-fluorophenyl)methanone (3ab). Yellow solid; MP: 118−120 °C; yield: 97%; ^{1}H NMR (500 MHz, $CDCl_3$) δ 9.07 (s, 1H, Ar−H), 7.73 (t, J = 9.3 Hz, 2H, Ar−H), 7.53 (d, J = 9.0 Hz, 1H, Ar−H), 7.43 (td, J = 8.0, 5.7 Hz, 1H, Ar−H), 7.26 (s, 1H, Ar−H), 7.24 (s, 1H, Ar−H), 7.20 (dd, J = 8.9, 1.5 Hz, 2H, Ar−H), 7.16 (d, J = 8.0 Hz, 2H, Ar−H), 5.73 (dd, J = 11.6, 4.8 Hz, 1H, CH), 3.98 (dd, J = 17.1, 11.6 Hz, 1H, CH_2), 3.42 (dd, J = 17.1, 4.8 Hz, 1H, CH_2), 2.60 (s, 3H, CH_3), 2.31 (s, 3H, CH_3), 2.27 (s, 3H, CH_3); ^{13}C NMR (100 MHz, $CDCl_3$) δ 165.05, 163.07, 161.12, 148.10, 147.71, 145.42, 138.54, 137.87, 137.36, 137.30, 130.19, 129.86, 129.54, 129.47, 126.75, 125.79, 125.31, 123.94, 117.79, 117.62, 116.71, 116.52, 115.76, 59.37, 44.36, 21.23 (CH_3), 18.29 (CH_3), 16.30 (CH_3); mass spectra: calculated for $C_{26}H_{23}FN_4O$: 426.1856, observed: 428.2122 $[M+2H]^+$.

(3-(2,6-Dimethylimidazo[1,2-a]pyridin-3-yl)-5-(3-hydroxy-4-methoxyphenyl)-4,5-dihydro-1H-pyrazol-1-yl)(3-fluorophenyl)methanone (3ac). Yellow solid; MP: 146−148 °C; yield: 98%; ^{1}H NMR (500 MHz, $CDCl_3$): δ 9.02 (s, 1H, Ar−H), 8.01−7.78 (m, 1H, Ar−H), 7.80−7.68 (m, 2H, Ar−H), 7.57−7.38 (m, 3H, Ar−H), 7.29 (s, 1H, Ar−H), 7.34−7.10 (m, 2H, Ar−H), 5.73 (dd, J = 11.5, 4.5 Hz, 1H, CH), 3.97 (dd, 17.0, 12.0 Hz, 1H, CH_2), 3.82 (s, 3H, OCH_3), 3.44 (s, 1H, CH_2), 2.60 (s, 3H, CH_3), 2.25 (s, 3H, CH_3); ^{13}C NMR (100 MHz, $CDCl_3$) δ 165.12, 163.07, 161.65, 161.11, 151.04, 147.79, 140.18, 134.09, 130.30, 130.24, 130.13, 129.56, 129.51, 129.45, 126.73, 126.17, 125.37, 125.02, 123.87, 120.82, 120.65, 117.89, 117.74, 115.80, 115.71, 112.96, 111.61, 111.05, 58.85 (CH), 56.15 (OCH_3), 44.09 (CH_2), 18.27 (CH_3), 16.42 (CH_3); mass spectra: calculated for $C_{26}H_{23}FN_4O_3$ = 458.1800; observed = 459.2380 $[M + H]^+$.

(3-(2,6-Dimethylimidazo[1,2-a]pyridin-3-yl)-5-(3-hydroxyphenyl)-4,5-dihydro-1H-pyrazol-1-yl)(3-fluorophenyl)-methanone (3ad). White solid; MP: 98−100 °C; yield: 98%; ^{1}H NMR (500 MHz, $CDCl_3$): δ 9.18 (s, 1H, Ar−H), 8.04−7.88 (m, 2H, Ar−H), 7.81 (d, J = 9 Hz, 1H, Ar−H), 7.75−7.59 (m, 2H, Ar−H), 7.54 (d, J = 8.0 Hz, 1H, Ar−H), 7.53−7.40 (m, 2H, Ar−H), 7.28 (d, J = 9.0 Hz, 1H, Ar−H), 5.83 (dd, J = 11.5, 5.5 Hz, 1H, CH), 4.06 (dd, J = 15.5, 11.0 Hz, 1H, CH_2), 3.49 (dd, J = 17.0, 5.0 Hz, 1H, CH_2), 2.76 (s, 3H, CH_3), 2.31 (s, 3H, CH_3); ^{13}C NMR (100 MHz, $CDCl_3$) δ 163.99, 163.09, 161.67, 161.13, 145.89, 142.41, 136.57, 136.51, 134.66, 130.46, 130.40, 129.92, 129.86, 127.69, 127.36, 126.04, 125.27, 123.61, 121.75, 121.09, 120.92, 119.19, 118.37, 118.20, 117.21, 117.03, 116.58, 116.39, 113.47, 59.61, 43.93, 18.34, 13.46; mass spectra: calculated for $C_{26}H_{23}FN_4O_3$ = 428.1649; observed = 429.1454 $[M + H]^+$.

(3-(2,6-Dimethylimidazo[1,2-a]pyridin-3-yl)-5-(3-methoxyphenyl)-4,5-dihydro-1H-pyrazol-1-yl)(3-fluorophenyl)-methanone (3ae). Yellow solid; MP: 98−100 °C; yield: 97%; ^{1}H NMR (500 MHz, $CDCl_3$): δ 9.07 (s, 1H, Ar−H), 7.80−7.67 (m, 2H, Ar−H), 7.54 (d, J = 9.0 Hz, 1H, Ar−H), 7.52−7.37 (m, 1H, Ar−H), 7.35−7.21 (m, 1H, Ar−H), 7.27−7.15 (m, 2H, Ar−H), 6.94 (d, J = 8.0 Hz, 1H, Ar−H), 6.88 (s, 1H, Ar−H), 6.88−6.76 (m, 1H, Ar−H), 5.73 (dd, J = 11.5, 4.5 Hz, 1H, CH), 3.99 (dd, J = 17.0, 11.5 Hz, 1H, CH_2), 3.78 (s, 3H, OCH_3), 3.42 (dd, J = 17.0, 5.0 Hz, 1H, CH_2), 2.60 (s, 3H, CH_3), 2.27 (s, 3H, CH_3); ^{13}C NMR (100 MHz, $CDCl_3$) δ 165.13, 163.09, 161.13, 160.20, 147.94, 147.64, 145.30, 143.03, 137.24, 137.18, 130.39, 130.33, 129.58, 129.52, 126.77, 125.32, 124.05, 117.89, 117.70, 116.71, 116.53, 115.69, 113.58, 113.00, 111.90, 59.49 (CH), 55.36 (OCH_3), 44.33 (CH_2), 18.29 (CH_3), 16.24 (CH_3); mass spectra: calculated for $C_{26}H_{23}FN_4O_2$ = 442.1800; observed = 443.2464 $[M + H]^+$.

(3-(2,6-Dimethylimidazo[1,2-a]pyridin-3-yl)-5-phenyl-4,5-dihydro-1H-pyrazol-1-yl)(3-fluorophenyl)methanone (3af). Yellow solid; MP: 108−110 °C; yield: 97%; ^{1}H NMR (500 MHz, $CDCl_3$): δ 9.08 (s, 1H, Ar−H), 7.81−7.67 (m, 2H, Ar−H), 7.53 (d, J = 9.0 Hz, 1H, Ar−H), 7.49−7.37 (m, 1H, Ar−H), 7.41−7.31 (d, J = 4.4 Hz, 4H, Ar−H), 7.29 (d, J = 4.4 Hz, 1H, Ar−H), 7.23−7.21 (m, 1H, Ar−H), 7.20 (s, 1H, Ar−H), 5.77 (dd, J = 11.6, 4.8 Hz, 1H, CH), 4.01 (dd, J = 17.1, 11.7 Hz, 1H, CH_2), 3.44 (dd, J = 17.1, 4.9 Hz, 1H, CH_2), 2.60 (s, 3H, CH_3), 2.27 (s, 3H, CH_3); ^{13}C NMR (100 MHz, $CDCl_3$) δ 165.09, 163.08, 161.13, 148.25, 147.71, 145.52, 141.44, 137.28, 137.23, 130.15, 129.56, 129.50, 129.22, 128.11, 126.74, 125.84, 125.33, 123.91, 117.84, 117.68, 116.73, 116.55, 115.81, 113.56, 59.56, 44.34, 18.29, 16.37; mass spectra: calculated for $C_{25}H_{21}FN_4O$ = 412.1700; observed = 413.2194 $[M + H]^+$.

Cell Lines and Cell Viability Assay. The cell viability assay was performed using AlamarBlue (Invitrogen, DAL1025, US). Briefly, 2×10^3 MCF-7 cells were seeded in 96-well plates and treated with 10-fold serial diluted concentrations of the compounds (0.001, 0.01, 0.1, 1.0, 10.0, and 100.0 μM) or control medium RPMI 1640 (Gibco,11875093, US) supplemented with 2% FBS (cell-box, CF-01S-02, China) maintained at 37 °C in a humidified 5% CO_2 incubator for 72 h, respectively. After treatment, cells were washed with phosphate buffered saline (PBS) and incubated for 4 h in 0.2 mL of 10% AlamarBlue solution at 37 °C in 5% CO in an incubator. Next, fluorescence was determined at an excitation wavelength of 575 nm and an emission wavelength of 595 nm using a Tecan

https://doi.org/10.1021/acsomega.3c10504
ACS Omega 2025, 10, 114−126

microplate reader. The viability of cells cultured in the presence of the assessed compounds was calculated as a percentage of the control cells, and the IC_{50} values were obtained from dose−response curves. All experiments were performed with triplicate determinations, and the IC_{502} was calculated using GraphPad Software 10.0 (GraphPad Inc., San Diego, CA, USA).

Molecular Docking. Molecular docking simulation was performed using AutoDock4 tools.[57] Initially, the crystal structure of STAT3 (PDB ID: 1BG1) was retrieved from the Protein Data Bank. The protein structure was prepared by removing water molecules and heteroatoms. Hydrogen atoms were added by using BIOVIA Discovery Studio software.[58] Later, ligand preparation was performed and the three-dimensional structure of **3p** was generated and optimized using suitable software. Ligand was assigned partial charges and saved in PDBQT format. AutoDock4 tools were employed to perform molecular docking simulations. The grid box was generated for **3p** with grid dimensions of 40 Å × 40 Å × 40 Å and a spacing of 0.453 Å. The Lamarckian Genetic Algorithm (LGA) was used to search for favorable binding modes of **3p** within the STAT3. The number of genetic algorithm runs was set to 10, and other parameters were kept at default settings. Later, the docking results were visualized using AutoDock, Discovery Studio, and UCSF Chimera.[59]

Western Blot Analysis. Briefly, cells were lysed in RIPA buffer and proteins in the cell lysate were resolved using SDS polyacrylamide gel electrophoresis, the proteins were transferred on a PVDF membrane following electrophoresis, blocked with 5% BSA blocking buffer (5g BSA in 50 ML TBST), and probed with different antibodies (1:1000) overnight at 4 °C. After a 1 h exposure to horseradish peroxidase (HRP)-conjugated secondary antibodies, the blot was washed and analyzed using chemiluminescence, and visualized by ChemiDoc Touch (BIO-RAD, USA) with Clarity and Clarity Max Western ECL Blotting Substrates (BIO-RAD, USA). The primary antibodies used are tabulated as below. The secondary antirabbit, antimouse, and antigoat horseradish peroxidase (HRP)-conjugated antibodies were obtained from Cell Signaling Technology (MA USA).

Live/Dead Cells Assay. Live/dead cells visualization was performed as per manufacturer's instructions using LIVE/DEAD Cell Imaging Kit (Thermo Fisher Scientific, USA), IF analyses were performed as previously described[60] using confocal microscopy (C2+, Nikon, Japan). Microscopic visualization of calcein-AM (green) stained colonies (live) and BOBO-3 iodide (red) stained cell debris (dead) after exposure to **3p**. Scale bars, 100 μm.

CONCLUSIONS

In conclusion, newer imidazo[1,2-*a*]pyridine clubbed pyrazolines **2**(**a-o**) and derivatives **3**(**a-af**) have been synthesized and evaluated for efficacy in producing loss of viability of MCF-7 cells. Among the series, compounds **3n** and **3p** are more potent with IC_{50} values of 55 and 15 nM, respectively. In silico docking analysis of compound **3p** predicted that **3p** bound to STAT3 protein with a higher binding energy of −9.57 kcal/mol. Furthermore, compound **3p** inhibited pSTAT3 levels in MCF-7 and T47D cells in a dose-dependent manner. Additionally, live/dead assay revealed that compound **3p** produced significant cell death in MCF-7 and T47D cells. In summary, the synthesis of imidazo[1,2-*a*]pyridine clubbed pyrazoline derivatives which are efficacious in ER+ BC cells, serving as inhibitors of STAT3 phosphorylation, is reported. The novel drug structures offer avenues to develop therapeutic approaches that may be useful in BC, either alone or in combination with other therapeutic modalities.

ASSOCIATED CONTENT

Supporting Information

The Supporting Information is available free of charge at https://pubs.acs.org/doi/10.1021/acsomega.3c10504.

Figures S1−S131: spectral data of **2**(**a**−**o**) and **3**(**a**−**af**); Figure S133: IC_{50} values of **2**(**a**−**o**) and **3**(**a**−**af**); Figure S134: original Western blot data of **3p** (PDF)

AUTHOR INFORMATION

Corresponding Authors

Vijay Pandey − *Institute of Biopharmaceutical and Health Engineering, Tsinghua Shenzhen International Graduate School, Tsinghua University, Shenzhen 518055, China*; Email: vijay.pandey@sz.tsinghua.edu.cn

Basappa Basappa − *Laboratory of Chemical Biology, Department of Studies in Organic Chemistry, University of Mysore, Mysore, Karnataka 570006, India*; orcid.org/0000-0002-8844-468X; Email: salundibasappa@gmail.com

Authors

Tejaswini P. Siddappa − *Laboratory of Chemical Biology, Department of Studies in Organic Chemistry, University of Mysore, Mysore, Karnataka 570006, India*; orcid.org/0009-0006-8763-7689

Akshay Ravish − *Laboratory of Chemical Biology, Department of Studies in Organic Chemistry, University of Mysore, Mysore, Karnataka 570006, India*

Zhang Xi − *Shenzhen Bay Laboratory, Shenzhen 518055, China*; orcid.org/0000-0003-4093-0897

Arunkumar Mohan − *Laboratory of Chemical Biology, Department of Studies in Organic Chemistry, University of Mysore, Mysore, Karnataka 570006, India*; orcid.org/0009-0009-2058-8386

Swamy S. Girimanchanaika − *Laboratory of Chemical Biology, Department of Studies in Organic Chemistry, University of Mysore, Mysore, Karnataka 570006, India*

Niranjan Pattehali Krishnamurthy − *NMR Research Centre, Indian Institute of Science, Bangalore, Karnataka 560012, India*

Shreeja Basappa − *Department of Chemistry, BITS-Pilani Hyderabad Campus, Medchal 500078, India*

Santosh L. Gaonkar − *Department of Chemistry, Manipal Institute of Technology, Manipal Academy of Higher Education, Manipal, Karnataka 576104, India*

Peter E. Lobie − *Shenzhen Bay Laboratory, Shenzhen 518055, China; Institute of Biopharmaceutical and Health Engineering, Tsinghua Shenzhen International Graduate School, Tsinghua University, Shenzhen 518055, China*

Complete contact information is available at: https://pubs.acs.org/10.1021/acsomega.3c10504

Author Contributions

○T.P.S. and A.R. contributed equally to this work. T.P.S., A.R., Z.X., A.M., S.S.G., S.B., and B.B. contributed to conceptualization, methodology, formal analysis, and writing; S.L.G. and N.P.K. contributed to formal analysis; V.P. and P.E.L.

https://doi.org/10.1021/acsomega.3c10504
ACS Omega 2025, 10, 114−126

contributed to methodology, writing, and editing; and B.B. contributed to conceptualization, methodology, software, data curation, original draft, validation, writing, and editing. All authors have read and agreed to the published version of the manuscript.

Notes

The authors declare no competing financial interest.

■ ACKNOWLEDGMENTS

This work was supported by the Vision Group on Science and Technology (CESEM) and the Government of Karnataka. This research was further supported by the National Natural Science Foundation of China (82172618); the Shenzhen Key Laboratory of Innovative Oncotherapeutics (ZDSYS20200820165400003) (Shenzhen Science and Technology Innovation Commission), China; Universities Stable Funding Key Projects (WDZC20200821150704001), China; the Shenzhen Bay Laboratory, Oncotherapeutics (21310031), China; and the National Key R & D Program of China (2023YFA0913602). A.R. was supported by the KSTePS fellowship, Karnataka.

■ ABBREVIATIONS

STAT	signal transduction and activation of transcription
pSTAT	phosphorylated signal transduction and activation of transcription
NMR	nuclear magnetic resonance
TLC	thin layer chromatography

■ REFERENCES

(1) Giaquinto, A. N.; Sung, H.; Miller, K. D.; Kramer, J. L.; Newman, L. A.; Minihan, A.; Jemal, A.; Siegel, R. L. Breast Cancer Statistics, 2022. *CA Cancer J. Clin.* **2022**, *72* (6), 524−541.

(2) Falzone, L.; Salomone, S.; Libra, M. Evolution of Cancer Pharmacological Treatments at the Turn of the Third Millennium. *Front. Pharmacol.* **2018**, *9*, 1300.

(3) Schirrmacher, V. From Chemotherapy to Biological Therapy: A Review of Novel Concepts to Reduce the Side Effects of Systemic Cancer Treatment (Review). *Int. J. Oncol.* **2018**, *54*, 407−419.

(4) Anand, U.; Dey, A.; Chandel, A. K. S.; Sanyal, R.; Mishra, A.; Pandey, D. K.; De Falco, V.; Upadhyay, A.; Kandimalla, R.; Chaudhary, A.; et al. Cancer Chemotherapy and beyond: Current Status, Drug Candidates, Associated Risks and Progress in Targeted Therapeutics. *Genes Dis.* **2023**, *10* (4), 1367−1401.

(5) van den Boogaard, W. M. C.; Komninos, D. S. J.; Vermeij, W. P. Chemotherapy Side-Effects: Not All DNA Damage Is Equal. *Cancers* **2022**, *14*, 627.

(6) Senapati, S.; Mahanta, A. K.; Kumar, S.; Maiti, P. Controlled Drug Delivery Vehicles for Cancer Treatment and Their Performance. *Signal Transduction Targeted Ther.* **2018**, *3* (1), 7.

(7) Tolomeo, M.; Cascio, A. The Multifaced Role of STAT3 in Cancer and Its Implication for Anticancer Therapy. *Int. J. Mol. Sci.* **2021**, *22*, 603.

(8) Bousoik, E.; Montazeri Aliabadi, H. "Do We Know Jack" About JAK? A Closer Look at JAK/STAT Signaling Pathway. *Front. Oncol.* **2018**, *8*, 287.

(9) Awasthi, N.; Liongue, C.; Ward, A. C. STAT Proteins: A Kaleidoscope of Canonical and Non-Canonical Functions in Immunity and Cancer. *J. Hematol. Oncol.* **2021**, *14* (1), 198.

(10) Furtek, S. L.; Backos, D. S.; Matheson, C. J.; Reigan, P. Strategies and Approaches of Targeting STAT3 for Cancer Treatment. *ACS Chem. Biol.* **2016**, *11*, 308−318.

(11) Malojirao, V. H.; Girimanchanaika, S. S.; Shanmugam, M. K.; Sherapura, A.; Dukanya; Metri, P. K.; Vigneshwaran, V.; Chinnathambi, A.; Alharbi, S. A.; Rangappa, S.; et al. Novel 1,3,4-Oxadiazole Targets STAT3 Signaling to Induce Antitumor Effect in Lung Cancer. *Biomedicines* **2020**, *8* (9), 368.

(12) Sethi, G.; Chatterjee, S.; Rajendran, P.; Li, F.; Shanmugam, M. K.; Wong, K. F.; Kumar, A. P.; Senapati, P.; Behera, A. K.; Hui, K. M.; et al. Inhibition of STAT3 Dimerization and Acetylation by Garcinol Suppresses the Growth of Human Hepatocellular Carcinoma in Vitro and in Vivo. *Mol. Cancer* **2014**, *13* (1), 66.

(13) Arora, L.; Kumar, A.; Arfuso, F.; Chng, W.; Sethi, G. The Role of Signal Transducer and Activator of Transcription 3 (STAT3) and Its Targeted Inhibition in Hematological Malignancies. *Cancers* **2018**, *10*, 327.

(14) Mohan, C. D.; Rangappa, S.; Preetham, H. D.; Chandra Nayaka, S.; Gupta, V. K.; Basappa, S.; Sethi, G.; Rangappa, K. S. Targeting STAT3 Signaling Pathway in Cancer by Agents Derived from Mother Nature. *Semin. Cancer Biol.* **2022**, *80*, 157−182.

(15) Ma, J.; Qin, L.; Li, X. Role of STAT3 Signaling Pathway in Breast Cancer. *Cell Commun. Signal.* **2020**, *18* (1), 33.

(16) Mohankumar, K. M.; Perry, J. K.; Kannan, N.; Kohno, K.; Gluckman, P. D.; Emerald, B. S.; Lobie, P. E. Transcriptional Activation of Signal Transducer and Activator of Transcription (STAT) 3 and STAT5B Partially Mediate Homeobox A1-Stimulated Oncogenic Transformation of the Immortalized Human Mammary Epithelial Cell. *Endocrinology* **2008**, *149*, 2219−2229.

(17) Manore, S. G.; Doheny, D. L.; Wong, G. L.; Lo, H.-W. IL-6/JAK/STAT3 Signaling in Breast Cancer Metastasis: Biology and Treatment. *Front. Oncol.* **2022**, *12*, 14.

(18) Wang, H.; Man, Q.; Huo, F.; Gao, X.; Lin, H.; Li, S.; Wang, J.; Su, F.; Cai, L.; Shi, Y.; et al. STAT3 Pathway in Cancers: Past, Present, and Future. *MedComm* **2022**, *3* (2), No. e124.

(19) Hu, X.; Li, J.; Fu, M.; Zhao, X.; Wang, W. The JAK/STAT Signaling Pathway: From Bench to Clinic. *Signal Transduction Targeted Ther.* **2021**, *6* (1), 402.

(20) Seif, F.; Khoshmirsafa, M.; Aazami, H.; Mohsenzadegan, M.; Sedighi, G.; Bahar, M. The Role of JAK-STAT Signaling Pathway and Its Regulators in the Fate of T Helper Cells. *Cell Commun. Signal.* **2017**, *15* (1), 23.

(21) Jung, Y. Y.; Ha, I. J.; Um, J.-Y.; Sethi, G.; Ahn, K. S. Fangchinoline Diminishes STAT3 Activation by Stimulating Oxidative Stress and Targeting SHP-1 Protein in Multiple Myeloma Model. *J. Adv. Res.* **2022**, *35*, 245−257.

(22) Jampilek, J. Heterocycles in Medicinal Chemistry. *Molecules* **2019**, *24*, 3839.

(23) Taylor, A. P.; Robinson, R. P.; Fobian, Y. M.; Blakemore, D. C.; Jones, L. H.; Fadeyi, O. Modern Advances in Heterocyclic Chemistry in Drug Discovery. *Org. Biomol. Chem.* **2016**, *14*, 6611−6637.

(24) Kumar, V.; Kaur, K.; Gupta, G. K.; Sharma, A. K. Pyrazole Containing Natural Products: Synthetic Preview and Biological Significance. *Eur. J. Med. Chem.* **2013**, *69*, 735−753.

(25) Kumar, R.; Singh, H.; Mazumder, A.; Salahuddin; Yadav, R. K. Synthetic Approaches, Biological Activities, and Structure−Activity Relationship of Pyrazolines and Related Derivatives. *Top. Curr. Chem.* **2023**, *381* (3), 12.

(26) Bennani, F. E.; Doudach, L.; Cherrah, Y.; Ramli, Y.; Karrouchi, K.; Ansar, M.; Faouzi, M. E. A. Overview of Recent Developments of Pyrazole Derivatives as an Anticancer Agent in Different Cell Line. *Bioorg. Chem.* **2020**, *97*, 103470.

(27) Kong, Y.; Liu, S.; Wang, S.; Yang, B.; He, W.; Li, H.; Yang, S.; Wang, G.; Dong, C. Design, synthesis and anticancer activities evaluation of novel pyrazole modified catalpol derivatives. *Sci. Rep.* **2023**, *13* (1), 7756.

(28) Shaw, A. T.; Kim, D.-W.; Nakagawa, K.; Seto, T.; Crinó, L.; Ahn, M.-J.; De Pas, T.; Besse, B.; Solomon, B. J.; Blackhall, F.; et al.et al. Crizotinib versus Chemotherapy in Advanced ALK-Positive Lung Cancer. *N. Engl. J. Med.* **2013**, *368*, 2385−2394.

(29) Michel, B.; Grima, M.; Barthelmebs, M.; Imbs, J.-L. Mechanism of the Diuretic Effect of Muzolimine. *Eur. J. Pharmacol.* **1990**, *183* (3), 1058−1059.

(30) Dowling, G.; Malone, E. Analytical Strategy for the Confirmatory Analysis of the Non-Steroidal Anti-Inflammatory

https://doi.org/10.1021/acsomega.3c10504
ACS Omega 2025, 10, 114−126

Drugs Firocoxib, Propyphenazone, Ramifenazone and Piroxicam in Bovine Plasma by Liquid Chromatography Tandem Mass Spectrometry. *J. Pharm. Biomed. Anal.* **2011**, *56* (2), 359−365.
(31) Lees, P.; Toutain, P.-L. Pharmacokinetics Pharmacodynamics MetabolismToxicology and Residues of Phenylbutazone in Humans and Horses. *Vet. J.* **2013**, *196* (3), 294−303.
(32) Borges, R. S.; Palheta, I. C.; Ota, S. S. B.; Morais, R. B.; Barros, V. A.; Ramos, R. S.; Silva, R. C.; Costa, J. D. S.; Silva, C. H. T. P.; Campos, J. M.; Santos, C. B Toward of Safer Phenylbutazone Derivatives by Exploration of Toxicity Mechanism. *Molecules* **2019**, *24* (1), 143.
(33) Bouchette, D.; Akhondi, H.; Quick, J. Zolpidem. In *StatPearls [Internet]*; StatPearls Publishing: Treasure Island (FL), 2023. https://www.ncbi.nlm.nih.gov/books/NBK442008/.
(34) Mazzon, E.; Esposito, E.; Di Paola, R.; Impellizzeri, D.; Bramanti, P.; Cuzzocrea, S. Olprinone, a Specific Phosphodiesterase (PDE)-III Inhibitor, Reduces the Development of Multiple Organ Dysfunction Syndrome in Mice. *Pharmacol. Res.* **2011**, *64* (1), 68−79.
(35) Murmann, W.; Carminati, G. M.; Cattaneo, R. Pharmacology of zolimidine (2-(p-methylsulfonylphenyl)-imidazo (1,2-*a*) pyridine) a new non-anticholinergic gastroprotective agent. III). Gastric antisecretory activity, antagonism against acid hypersecretion induced by pentagastrin and histamine, and other effects. *Panminerva Med.* **1974**, *16*, 335−346.
(36) He, L.-J.; Yang, D.-L.; Chen, H.-Y.; Huang, J.-H.; Zhang, Y.-J.; Qin, H.-X.; Wang, J.-L.; Tang, D.-Y.; Chen, Z.-Z. A Novel Imidazopyridine Derivative Exhibits Anticancer Activity in Breast Cancer by Inhibiting Wnt/β-catenin Signaling. *OncoTargets Ther.* **2020**, *13*, 10111−10121.
(37) Meenakshisundaram, S.; Manickam, M.; Pillaiyar, T. Exploration of Imidazole and Imidazopyridine Dimers as Anticancer Agents: Design, Synthesis, and Structure-Activity Relationship Study. *Arch. Pharm.* **2019**, *352*, 1900011.
(38) Sucu, B. O. Biological Evaluation of Imidazopyridine Derivatives as Potential Anticancer Agents against Breast Cancer Cells. *Med. Chem. Res.* **2022**, *31*, 2231−2242.
(39) Su, J.-C.; Chang, C.-H.; Wu, S.-H.; Shiau, C.-W. Novel Imidazopyridine Suppresses STAT3 Activation by Targeting SHP-1. *J. Enzyme Inhib. Med. Chem.* **2018**, *33*, 1248−1255.
(40) Zheng, Q.; Dong, H.; Mo, J.; Zhang, Y.; Huang, J.; Ouyang, S.; Shi, S.; Zhu, K.; Qu, X.; Hu, W.; et al.et al. A Novel STAT3 Inhibitor W2014-S Regresses Human Non-Small Cell Lung Cancer Xenografts and Sensitizes EGFR-TKI Acquired Resistance. *Theranostics* **2021**, *11*, 824−840.
(41) Liu, D.; Hu, G.; Long, G.; Qiu, H.; Mei, Q.; Hu, G. Celecoxib Induces Apoptosis and Cell-Cycle Arrest in Nasopharyngeal Carcinoma Cell Lines via Inhibition of STAT3 Phosphorylation. *Acta Pharmacol. Sin.* **2012**, *33*, 682−690.
(42) Zhang, L.; Peterson, T. E.; Lu, V. M.; Parney, I. F.; Daniels, D. J. Antitumor Activity of Novel Pyrazole-Based Small Molecular Inhibitors of the STAT3 Pathway in Patient Derived High Grade Glioma Cells. *PLoS One* **2019**, *14*, No. e0220569.
(43) LaPorte, M. G.; Wang, Z.; Colombo, R.; Garzan, A.; Peshkov, V. A.; Liang, M.; Johnston, P. A.; Schurdak, M. E.; Sen, M.; Camarco, D. P.; et al.et al. Optimization of Pyrazole-Containing 1,2,4-Triazolo-[3,4-b]Thiadiazines, a New Class of STAT3 Pathway Inhibitors. *Bioorg. Med. Chem. Lett.* **2016**, *26* (15), 3581−3585.
(44) Wang, F.; Feng, K.-R.; Zhao, J.-Y.; Zhang, J.-W.; Shi, X.-W.; Zhou, J.; Gao, D.; Lin, G.-Q.; Tian, P. Identification of Novel STAT3 Inhibitors Bearing 2-Acetyl-7-Phenylamino Benzofuran Scaffold for Antitumour Study. *Bioorg. Med. Chem.* **2020**, *28* (24), 115822.
(45) Ravish, A.; Shivakumar, R.; Xi, Z.; Yang, M. H.; Yang, J.-R.; Swamynayaka, A.; Nagaraja, O.; Madegowda, M.; Chinnathambi, A.; Alharbi, S. A.; et al.et al. De Novo Design of Imidazopyridine-Tethered Pyrazolines That Target Phosphorylation of STAT3 in Human Breast Cancer Cells. *Bioengineering* **2023**, *10*, 159.
(46) Anilkumar, N. C.; Sundaram, M. S.; Mohan, C. D.; Rangappa, S.; Bulusu, K. C.; Fuchs, J. E.; Girish, K. S.; Bender, A.; Basappa; Rangappa, K. S. A One Pot Synthesis of Novel Bioactive Tri-Substitute-Condensed-Imidazopyridines That Targets Snake Venom Phospholipase A2. *PLoS One* **2015**, *10* (7), No. e0131896.
(47) Hua, Y.; Yuan, X.; Shen, Y.; Wang, J.; Azeem, W.; Yang, S.; Gade, A.; Lellahi, S. M.; Øyan, A. M.; Ke, X.; et al. Novel STAT3 Inhibitors Targeting STAT3 Dimerization by Binding to the STAT3 SH2 Domain. *Front. Pharmacol.* **2022**, *13*, 836724.
(48) Kong, R.; Bharadwaj, U.; Eckols, T. K.; Kolosov, M.; Wu, H.; Cruz-Pavlovich, F. J. S.; Shaw, A.; Ifelayo, O. I.; Zhao, H.; Kasembeli, M. M.; et al. Novel STAT3 Small-Molecule Inhibitors Identified by Structure-Based Virtual Ligand Screening Incorporating SH2 Domain Flexibility. *Pharmacol. Res.* **2021**, *169*, 105637.
(49) Chen, X.; Vinkemeier, U.; Zhao, Y.; Jeruzalmi, D.; Darnell, J. E.; Kuriyan, J. Crystal Structure of a Tyrosine Phosphorylated STAT-1 Dimer Bound to DNA. *Cell* **1998**, *93* (5), 827−839.
(50) Sgrignani, J.; Garofalo, M.; Matkovic, M.; Merulla, J.; Catapano, C. V.; Cavalli, A. Structural Biology of STAT3 and Its Implications for Anticancer Therapies Development. *Int. J. Mol. Sci.* **2018**, *19*, 1591.
(51) Dees, S.; Pontiggia, L.; Jasmin, J.-F.; Mercier, I. Phosphorylated STAT3 (Tyr705) as a Biomarker of Response to Pimozide Treatment in Triple-Negative Breast Cancer. *Cancer Biol. Ther.* **2020**, *21*, 506−521.
(52) Revanna, C. N.; Basappa; Srinivasan, V.; Li, F.; Kodappully, S. S.; Xiaoyun, D.; Shivananju, N. S.; Bhadregowda, D. G.; Gautam, S.; Mantelingu, K.; Andreas, B.; Rangappa, K. S. Synthesis and Biological Evaluation of Tetrahydropyridinepyrazoles ('PFPs') as Inhibitors of STAT3 Phosphorylation. *MedChemcomm* **2014**, *5*, 32.
(53) Mohan, C. D.; Bharathkumar, H.; Bulusu, K. C.; Pandey, V.; Rangappa, S.; Fuchs, J. E.; Shanmugam, M. K.; Dai, X.; Li, F.; Deivasigamani, A.; et al.et al. Development of a Novel Azaspirane That Targets the Janus Kinase-Signal Transducer and Activator of Transcription (STAT) Pathway in Hepatocellular Carcinoma *in Vitro* and *in Vivo*. *J. Biol. Chem.* **2014**, *289*, 34296−34307.
(54) LaPorte, M. G.; Wang, Z.; Colombo, R.; Garzan, A.; Peshkov, V. A.; Liang, M.; Johnston, P. A.; Schurdak, M. E.; Sen, M.; Camarco, D. P.; et al.et al. Optimization of Pyrazole-Containing 1,2,4-Triazolo-[3,4-b]Thiadiazines, a New Class of STAT3 Pathway Inhibitors. *Bioorg. Med. Chem. Lett.* **2016**, *26*, 3581−3585.
(55) Gutierrez, D. A.; Contreras, L.; Villanueva, P. J.; Borrego, E. A.; Morán-Santibañez, K.; Hess, J. D.; DeJesus, R.; Larragoity, M.; Betancourt, A. P.; Mohl, J. E.; et al.et al. Identification of a Potent Cytotoxic Pyrazole with Anti-Breast Cancer Activity That Alters Multiple Pathways. *Cells* **2022**, *11*, 254.
(56) Basappa, B.; Chumadathil Pookunoth, B.; Shinduvalli Kempasiddegowda, M.; Knchugarakoppal Subbegowda, R.; Lobie, P. E.; Pandey, V. Novel Biphenyl Amines Inhibit Oestrogen Receptor (ER)-α in ER-Positive Mammary Carcinoma Cells. *Molecules* **2021**, *26*, 783.
(57) Huey, R.; Morris, G. M.; Olson, A. J.; Goodsell, D. S. A Semiempirical Free Energy Force Field with Charge-Based Desolvation. *J. Comput. Chem.* **2007**, *28*, 1145−1152.
(58) BIOVIA Dassault Systèmes *Discovery Studio Visualizer*; Dassault Systèmes: San Diego, CA, USA, 2020; Vol. *21*.
(59) Pettersen, E. F.; Goddard, T. D.; Huang, C. C.; Couch, G. S.; Greenblatt, D. M.; Meng, E. C.; Ferrin, T. E. UCSF Chimera—A Visualization System for Exploratory Research and Analysis. *J. Comput. Chem.* **2004**, *25*, 1605−1612.
(60) Zhang, X.; Wang, L.; Chen, S.; Huang, P.; Ma, L.; Ding, H.; Basappa, B.; Zhu, T.; Lobie, P. E.; Pandey, V. Combined Inhibition of BADSer99 Phosphorylation and PARP Ablates Models of Recurrent Ovarian Carcinoma. *Commun. Med.* **2022**, *2* (1), 82.

https://doi.org/10.1021/acsomega.3c10504
ACS Omega 2025, 10, 114−126